Technical Report HCSU-093

HAWAIIAN HOARY BAT (*LASIURUS CINEREUS SEMOTUS*) BEHAVIOR AT WIND TURBINES ON MAUI

P. Marcos Gorresen[1], Paul M. Cryan[2], and Grace Tredinnick[1]

1 Hawai'i Cooperative Studies Unit, University of Hawai'i at Hilo, P.O. Box 44, Hawai'i National Park, HI 96718
2 U.S. Geological Survey, Fort Collins Science Center, 2150 Centre Avenue, Bldg. C, Fort Collins, CO 80526

Hawai'i Cooperative Studies Unit
University of Hawai'i at Hilo

200 W. Kawili St.
Hilo, HI 96720

(808) 933-0706

May 2020

USGS science for a changing world

UNIVERSITY of HAWAI'I® HILO

This product was prepared under Cooperative Agreement CAG15AC00203 for the Pacific Island Ecosystems Research Center of the U.S. Geological Survey.

TABLE OF CONTENTS

LIST OF TABLES

LIST OF FIGURES

ABSTRACT

This study examined the activity of the endemic Hawaiian hoary bat (*Lasiurus cinereus semotus*) at wind turbines operated by Auwahi Wind Energy, LLC, on southern Maui Island, from August to November 2018. The research was conducted to assess the potential effect of wind speed and turbine operation on bat presence and behavior and compared information obtained from both acoustic monitoring and thermal videography.

During the four months of nightly surveillance at four wind turbines, we observed 384 visual (videographic) and 244 acoustic detection events involving bats. Bats were infrequently detected, averaging 0.08 events per hour for both visual and acoustic samples. Detections occurred throughout the monitoring period, but bat presence was only evident for a fraction (acoustic: 30%; visual: 44%) of the turbine-nights sampled. Bats were present throughout the night, but detections exhibited a unimodal peak centered on the first third of the night, with events largely absent in the latter half of the night and no apparent seasonal trend towards earlier or later occurrence within nights. However, a decline in the visual detection rate was noted over the four-month period (a similar assessment was not available from acoustic samples due to missing data for much of the later months). Visual bat detections were not significantly correlated over nights (i.e., temporally), but were positively associated among turbines (i.e., spatially).

Visual detections were generally brief (median = 9.0 sec), infrequent (median time between events = 49.0 min), and involved single passes (57%) largely comprised of a single bat (94%). The amount of time during which bats were visually observed amounted to only 0.05% of total videographic monitoring (2.5 hours of 5,066 total hours). Although not directly comparable to the video results because of differences in the volume of airspace sampled and nature of observation, acoustic detection events were similarly brief (median = 6.0 sec), infrequent (median time between passes = 38.8 min), and also composed only 0.05% of the total period of acoustic monitoring (1.6 hours of 3,036 total hours). Most visual observations (61%) were of individuals flying at some point during the event to within about 15 m of the turbine nacelle (machinery housing atop the monopole). Erratic flight paths were the most prevalent flight type with bats often repeatedly approaching and circling the nacelle. Terminal-phase ("feeding buzz") calls were only noted in 3% of all acoustic events.

Bats were most frequently detected visually at relatively low wind speeds (median = 3.4 m/sec); however, 10% of events occurred at wind speeds over 8.5 m/sec. Nightly bat detection rates for the four-month period of monitoring were negatively correlated with total daily precipitation. Generalized linear mixed model analysis confirmed that detection rates were negatively associated with wind speed and precipitation and indicated a positive relation with intermittent wind speed and its consequent effect on turbine blade rotation (i.e., frequent intervals of starting and stopping).

The co-occurrence of bat detection obtained from videographic and acoustic monitoring methods was generally low, and in instances when individuals were visually observed, bats were detected acoustically during only 12% (within a 10-minute window), 22% (within a 2-hour window), and 56% (at some point during the entire night) of such events. Most visual detections (65% within a 2-hour window) lacking an acoustic detection involved bats observed flying within about 15 m of the turbine nacelle on which acoustic detector microphones were situated.

INTRODUCTION

The prevalence and causes of bird collisions with wind turbines have been studied and documented since the 1980s (e.g., Byrne 1983, Howell and Didonato 1991). Investigation into the scope of bat fatalities at wind energy facilities is a more recent development (e.g., Fiedler 2004, Johnson 2005, Kunz *et al.* 2007, Arnett *et al.* 2008). These studies have generally monitored bat acoustic activity at turbines to provide insight into the association of bat occurrence, turbine operation, and geographic and weather variables (e.g., Baerwald and Barclay 2009, Weller and Baldwin 2012, Foo *et al.* 2017).

Bats, however, are cryptic nocturnal mammals that can be difficult to sample during flight and at relevant heights. Recent research has found bats in flight may often forgo echolocation or vocalize in a way that is not detectable with common acoustic monitoring methods (Gorresen *et al.* 2017, Corcoran and Weller 2018). Silent flight behavior has implications for studies of bat behavior and management aimed at minimizing or avoiding fatalities associated with wind energy.

As an alternative to acoustic sampling, visual-based methods such as thermal imaging offer certain advantages due to its capacity to sample relatively large volumes of airspace over long periods and reveal aspects of bat behavior not readily obtained solely from acoustic data. To date, however, only a small number of studies have used thermal imaging to conduct long-term monitoring of bat behavior at wind turbines. These studies have shown bats engaged in investigative behavior of turbine blades, nacelles (machinery housing atop the monopole), and monopoles; repeated approaches after near strikes with moving blades; social interactions by multiple bats; and a concentration of flight activity on the leeward (downwind) side of turbines (Horn *et al.* 2008, Cryan *et al.* 2014, Gorresen *et al.* 2015b). Visual-based systems can produce higher detection probabilities than acoustic-only sampling (Gorresen *et al.* 2018) with the potential to improve assessments of bat activity and behavior at turbines (e.g., Korner-Nievergelt *et al.* 2013). However, although not relevant to Hawai'i (which harbors a single species of bat), video recordings are generally not informative for species identification.

Monitoring that combines both acoustic and visual-based systems may also have additional benefits in linking specific behaviors generally only evident when analyzed as paired data sources (e.g., response to deterrents [Gorresen *et al.* 2015a]; flight and vocalization indicative of foraging [Gorresen *et al.* 2018]; obstacle avoidance [Corcoran and Weller 2018]). Sampling with combined acoustic-visual systems may also help address questions related to the frequency of bat vocalization at turbines, a key consideration for management aimed at minimizing collision risk by curtailing turbine operation following the detection of vocalization (e.g., Hayes *et al.* 2019).

In light of the above, we initiated a study with support of Auwahi Wind Energy, LLC, that applied both acoustic and visual-based monitoring systems with the objective of examining bat behavior at wind turbines and its relation with wind speed, a principal variable in determining bat activity and collision risk at turbines (Korner-Nievergelt *et al.* 2013, Wellig *et al.* 2018). The Hawaiian hoary bat (*Lasiurus cinereus semotus*, Vespertilionidae) served as the focal species in this study because it is an endangered endemic susceptible to fatality by collision with moving wind turbine blades (Gorresen *et al.* 2015b) and the subject of management aimed at mitigating these effects (Mykleseth 2017, Tetra Tech 2018). The North American subspecies, *L. c. cinereus*, accounts for approximately 40% of all bat fatalities at turbines in continental North

America (Arnett and Baerwald 2013). Also known as the ʻŌpeʻapeʻa, the Hawaiian hoary bat is the only extant native terrestrial mammal and sole bat species in Hawaii State and occurs on all of the major islands (Tomich 1986). Given previous observations of cryptic vocalization by Hawaiian hoary bats in semi-natural environments (Gorresen *et al.* 2017), we also examined the correspondence between acoustic and visual-based detection rates of bats at wind turbines.

METHODS

Study Area

The study area was located on the wind energy facility operated by Auwahi Wind Energy, LLC, on southern Maui Island, Hawaii. Wind turbines at the facility consist of eight 3-megawatt WTGs (Siemens SWT-3.0-101, Hamburg, Germany), each with a hub height of 80 m, a rotor diameter of 101 m, a maximum height of 131 m, and a rotor-swept area of 8,012 m² (www.thewindpower.net/turbine_en_275_siemens_swt-3.0-101.php). Sampling for bat occurrence spanned a four-month period from August 1 to November 30, 2018, at four wind turbine generators (WTG 2, 4, 5, and 7) previously equipped with acoustic detectors managed by Natural Power Consultants, LLC (Saratoga Springs, New York, USA; described below).

Landcover in the area is dominated by dryland vegetation comprised of open grassland, wiliwili (*Erythrina sandwicensis*) groves, and kīawe (*Prosopis juliflora*). The moderately sloping area inclusive of the monitored turbines spans a low elevation range (150–315 m above sea level [asl]) near the coast and is situated over 7 km from tree vegetation that might serve as day-roost habitat (within the region, in areas generally >600 m asl).

Local climatic conditions in the area exhibit relatively constant temperatures, little rainfall, and persistent strong winds throughout much of the year. Sunset to sunrise (nighttime) temperature ranged from 29.1 to 25.9°C on August 1 and from 26.6 to 22.9°C on November 30 (recorded at a weather station located at sea-level 10.5 km west of the study area; www.wunderground.com/dashboard/pws/KHIKIHEI5; accessed December 3, 2018). Cumulative daily precipitation totaled 33.0 cm over the four-month study period (recorded at a weather station located 7.3 km east-northeast from the Auwahi Wind Energy facility [USGS 203721156151601 255.0 Kepuni Gulch Rain Gage; 225 m elevation] waterdata.usgs.gov/nwis/inventory?agency_code=USGS&site_no=203721156151601; accessed December 3, 2018; also available at https://doi.org/10.5066/F7P55KJN). Prevailing winds during this period were generally easterly, and nighttime wind speeds recorded at the nacelle (machinery housing atop the monopole) of sampled turbines averaged 7.1 m/sec (25.6 km/hr), with speeds above 13.0 m/sec recorded about 10% of the time (G. Akau, Auwahi Wind Energy, written comm., 2018). Wind speed and direction were recorded by an ultrasonic anemometer (FT702LT-V22, FT Technologies Ltd., Sunbury on Thames, United Kingdom) and adjusted for placement behind the rotors on a turbine nacelle. Wind speed data for the monitored turbines were provided by Auwahi Wind Energy.

Monitoring Bat Occurrence and Behavior

The rotor-swept area of each turbine was monitored using a surveillance camera equipped with a 19-mm lens (Axis Q1942-E, Axis Communications, Lund, Sweden) that imaged in the thermal infrared spectrum (~9,000–14,000 micrometers) of electromagnetic radiation. The camera sampled at a rate of 30 frames per second with a resolution of 640 by 480 pixels and required no supplemental illumination. The camera was mounted approximately 4 m from the ground on the turbine monopole using a mounting base (RigMount X6 Magnet Camera Mounting Platform,

Rigwheels, Minneapolis, Minnesota, USA; Figure 1). The camera was aimed directly up the tower such that the video scene included the monopole, turbine blades, nacelle, and surrounding airspace. Cameras were placed on the leeward (downwind) side of the turbines to image the perspective at which bat activity has been generally shown to be highest in prior studies (Cryan *et al.* 2014, Gorresen *et al.* 2015b).

Figure 1. Placement of camera on turbine monopole (circled, left panel) and camera orientation (right panel).

Video imagery was processed using custom-written code and matrix-based statistical software (Mathworks, Natick, Massachusetts, USA) to automatically detect animals flying through the video scenes. Video was recorded at 30 frames per second, and every 10th video frame was analyzed resulting in the detection of events lasting as little as 0.3 sec. All objects detected by software algorithms were visually reviewed and identified as bat, bird, or insect. Previous field trials showed that bats were detectable with thermal videography at distances of over 100 m.

Bat vocalization was acoustically monitored from atop turbines with acoustic detector systems (Batlogger WE X2, Elekon AG, Luzern, Switzerland) installed and managed by Natural Power Consultants, LLC (Saratoga Springs, New York, USA). Each turbine had one rotor-facing (windward) and one rear-facing (leeward) omnidirectional microphone mounted atop the nacelle and were each tipped down about 9 degrees from vertical. Detectors began recording

1 hour before local sunset until 1 hour after sunrise the next morning. Acoustic detections were recorded without digital compression as full-spectrum wav sound files with the following settings: sampling rate = 312.5 kHz; trigger frequency range of 9–60 kHz within a microphone sensitivity range of 10–150 kHz; decibel gain = 12; period trigger = 95; crest factor = 5; pre- and post-trigger duration = 500–800 ms; max gap time between calls = 200 ms; maximum call file duration = 3 sec; minimum FFT value for trigger = 5; minimum sound level for trigger = 1%. Microphone sensitivity tests were automatically conducted on a daily basis, and results were provided by Natural Power Consultants, LLC. Prevailing wind direction at the facility is usually from the east (80%; G. Akau, Auwahi Wind Energy, written comm., 2018); therefore, acoustic and video observations were expected to jointly sample the same airspace for approximately the same proportion of time.

Delays with acoustic detector installation atop turbines and the progressive decay of microphone sensitivity over the monitoring period limited the number of sample nights available for analyses. Microphone sensitivity was particularly problematic for the microphone aimed towards the rotor; consequently, with the exception of one analysis, only data for the rear-oriented microphone were examined herein. The periods during which acoustic data were determined to be available totaled to 246 nights (turbine 2, August 1–November 3 [63 nights]; turbine 4, September 20–October 6 [17 nights]; turbine 5, August 8–November 30 [115 nights]; turbine 7, August 7–September 26 [51 nights]). Moreover, because microphone sensitivity decayed as a function of time since installation, examination of acoustic detections relative to time of year was not possible because these variables were largely confounded. For these reasons, most descriptive analyses and the statistical modeling of bat occurrence and behavior relative to weather and turbine operation variables focused on thermal video-based detections. The exception was use of all acoustic wav files (i.e., both rotor- and rear-oriented) in an assessment of the correspondence of acoustic and visual (video) detections (the rationale being that this would minimize underestimation of the correspondence of both types of detections). The correspondence between acoustic and visual detection events were examined at three scales: the entire night (averaging approximately 12 hours), a 2-hour period (i.e., an acoustic detection 1 hour before or after a visual detection), and a 10-minute period (i.e., an acoustic detection 5 minutes before or after a visual detection). Bat passes at any point during a visual detection were noted if they occurred at a distance of approximately 15 m or less from the turbine nacelle, a range within which the probability of acoustic detection is high, particularly for low-frequency echolocation calls (Adams *et al.* 2012, Gorresen *et al*. 2017), and used to conservatively assess the proportion of visual detections lacking a corresponding acoustic detection.

Hawaiian hoary bat vocalizations were examined using Kaleidoscope Pro software (version 5.1.9, Wildlife Acoustics, Concord, Maine, USA). All echolocation pulses, feeding buzzes, and files with multiple bats were verified by audio and visual inspection, and all noise files were visually reviewed to ensure that bat calls were not missed. Terminal-phase calls ("feeding buzzes" emitted just prior to an attempted insect catch) were qualitatively distinguished from search and approach-phase calls by a rapid increase in the call rate. Ancillary information on the frequency of acoustic detection of bats from ground-based detectors in the region are described in Pinzari *et al.* (2019a), and for which acoustic data are available at https://doi.org/10.5066/P9U0KRMY (Pinzari *et al.* 2019b).

Videographic recordings were analyzed to identify individual "detection events", defined as a single pass or two or more detections occurring less than a minute apart, such that if bats went

out of video field-of-view they were not counted as independent events if they reappeared within 1 minute (consistent with previous work by Cryan *et al.* 2014 and Gorresen *et al.* 2018). Likewise, acoustic detections were also grouped as the same detection event when two or more passes occurred less than 1 minute apart. The resulting data for both video and acoustic sampling included total counts of detection events per night. In addition, to account for partially sampled nights or nights for which video was not available from one or more turbines, the nightly rate of bat detection (number of events per hour, adjusted for duration of night and sampling effort) was calculated both for individual turbines and all four turbines combined. Flight behavior was qualitatively designated as straight, curved, or erratic based on whether the flight path was linear or included one or more curves or loops during the video detection event. In cases where two or more bats were concurrently visible, behavior was recorded as agonistic when individuals flew within a few meters of each other and interacted with sharp turns and chases.

Variables Associated with Bat Detection

We examined the association of bat occurrence and behavior with several variables related to weather conditions and turbine operation. We hypothesized that nightly counts of detection events would be negatively related to wind speed and precipitation, as these conditions may restrict flight activity or foraging success (Erickson and West 2002). Conversely, we expected detections to be positively influenced by wind speed variability because high values of this variable reflect the recurrence of low wind periods during which bats may be more active or more likely to approach turbines. Moreover, the number of turbine blade rotation "start-ups" (i.e., from zero or low to high rates of rotation) has been found to be positively related to bat fatalities (Schirmacher *et al.* 2018), an outcome possibly linked to increased bat occurrence or activity at low wind speeds. The frequency of start-ups is generally associated with the incidence of wind speeds below that which triggers turbine shut-down and low-wind speed curtailment (LWSC; a management protocol for minimizing the likelihood of bat fatalities and incidental take). Consequently, high wind speed variability and frequent turbine start-ups are both variables expected to be positively related to nightly counts of detection events. Curtailment is accomplished by "feathering" turbine blades; that is, pitching blades parallel to the wind, resulting in very slow movement of the rotor and blades. During the period of study, turbine LWSC at Auwahi Wind Energy implemented a "cut-in speed" (i.e., wind speed at which the turbine begins to rotate and generate power) of 6.9 m/sec from August to October and 5 m/sec in November.

Wind speed (m/sec) recorded at the nacelle of each turbine at 10-minute intervals and limited to night-time periods were used to calculate nightly mean and standard deviation (SD) metrics; referred herein as "wind-mean" and "wind-sd". Turbine blade movement, measured as rotations per minute ("rpm"), was obtained for each turbine over 10-minute intervals from Auwahi Wind Energy. Turbine rpm during individual bat detection events were derived directly from the video recording of each event by calculating the time needed for the rotor to complete a full rotation. The frequency of turbine start-ups ("rpm-starts") was determined by tallying the number of times per night a turbine transitioned from ≤1 rpm to >1 rpm in two or more consecutive 10-minute periods. For context, at 1.0 rpm, blade tips are moving at a speed of 5.3 m/sec (= 19.0 km/hr) for a turbine rotor diameter of 101 m and a circumference of 317 m.

Precipitation was obtained from a weather station located 7.3 km east-northeast from the Auwahi Wind Energy facility (USGS site number 203721156151601, 255.0 Kepuni Gulch Rain Gage). Temperature was not included in analyses due to the low variability observed in

nighttime values over the four months of sampling (sunset to sunrise temperature differences averaged about 3.5°C).

Descriptive Analyses and Statistical Modeling

Bat occurrence and behavior were explored and graphically described with a variety of methods (e.g., analysis of variance, simple linear regression, correlation analysis) in the statistical computing environment R (version 3.5.1; R Core Team 2018). The relation of nightly counts of bat detection events to multiple predictor variables were also examined with generalized linear mixed models (GLMMs) using the glmmTMB package (Brooks*et al.* 2019) to account for temporally and spatially correlated observations requiring the incorporation of random effects. In the GLMMs the variables "night" and "turbine" were added as random effect terms to deal with repeated measures at the four turbines. In addition, the models were fit to counts for the following fixed effects: "rpm", "rpm-starts", "precip", "wind-mean", and "wind-sd". The fixed effect terms were scaled and centered on zero (creating z-scores) using the base scale function in R to improve model convergence and allow for direct comparison of the magnitude of fixed effect coefficients. Mean wind speed and turbine rpm were highly correlated ($r = 0.70$ from measures for all four turbines, and $r = 0.92$ when excluding turbine 2, which was not operational for most of the monitoring period). In addition, rpm start-ups and the standard deviation of wind during the night were also moderately correlated ($r = 0.37$). All other variables were correlated pairwise at an $r \leq 0.35$. Therefore, to minimize multicollinearity in regression analyses and limit the number of models tested, models were developed that did not jointly include both of the correlated variables. To account for differences in nightly sampling duration among turbines, we included the log of the total duration of recording per night and turbine as an offset in models, thereby converting counts of detection events to a detection rate.

Preliminary regression analyses demonstrated underdispersion of the residuals in both negative binomial and Poisson models. The consequence of underdispersion is that standard errors (SEs) are generally too conservative (i.e., confidence intervals tend to be too broad and p-values too large) potentially resulting in false-negative conclusions about parameter effects (Brooks*et al.* 2019). To address this, we fit GLMMs with several additional distribution specifications that allow for underdispersion; specifically, generalized Poisson and Conway-Maxwell-Poisson (Brooks*et al.* 2019). The four distribution groups are referred herein as NB, P, GP, and CMP for the negative binomial, Poisson, generalized Poisson, and Conway-Maxwell-Poisson models.

The candidate set of predictor variables totaled to 18 models, including a null model with only the random effect terms "night" and "turbine", the offset, and no fixed effects. We used small-sample-size corrected Akaike information criterion (AICc) via the AICctab function from the bbmle package (Burnham and Anderson 2002, Bolker and R Core Team 2017) to compare all models. Model ranking was performed in two steps: the first identified the top-ranked model from among the 18 candidate models within each of the four distribution groups (NB, P, GP, and CMP), and the second step ranked this subset. Final top-ranked models (i.e., those with a $\Delta AICc < 7$; Burnham *et al.* 2011) were examined with post-fitting diagnostics performed with the DHARMa package (Hartig 2017). A statistical significance criterion of $P < 0.05$ was used in all tests.

RESULTS

Visual (Thermal Video) Bat Detections—Descriptive Analyses

Thermal video was recorded at four turbines over the four-month period between August 1 and November 30, 2018. Technical difficulties resulted in the loss of recording for 65 turbine-nights. The number of nightly recordings over the 122-night period was 111, 119, 107, and 75 for turbines 2, 4, 5, and 7, respectively, for a total of 412 turbine-nights with a full or partial night of recording (median duration = 12.6 hours, including a 15-minute period before sunset and after sunrise). This yielded 5,066 hours of video that resulted in a total of 384 detection events of bats (72%) and bat-like observations (27%; n = 140) with an additional 288 bird observations. Only definitive bat detections were used in analyses of occurrence and behavior (i.e., bat-like detections were not included as these were generally brief and/or of distant targets). Visual bat detection data are available at https://doi.org/10.5066/P937H9LQ (Gorresen 2020) and are summarized in Appendix I and II.

Bats were detected visually in 44% (n = 180) of the turbine-nights sampled. Detections at turbines occurred throughout the night, with the earliest occurring 8 minutes after sunset and the latest 16 minutes before sunrise. Detections exhibited a unimodal distribution and a median of 0.27 for the fraction of night at which the observation occurred, corresponding to a peak of 3.4 hours after sunset (Q1 = 0.18, Q3 = 0.45, mean = 0.33 ± 0.20 SD; standardized as a fraction of night and scaled from 0 at sunset to 1 at sunrise; Figure 2). Detections generally did not begin until about an hour after sunset.

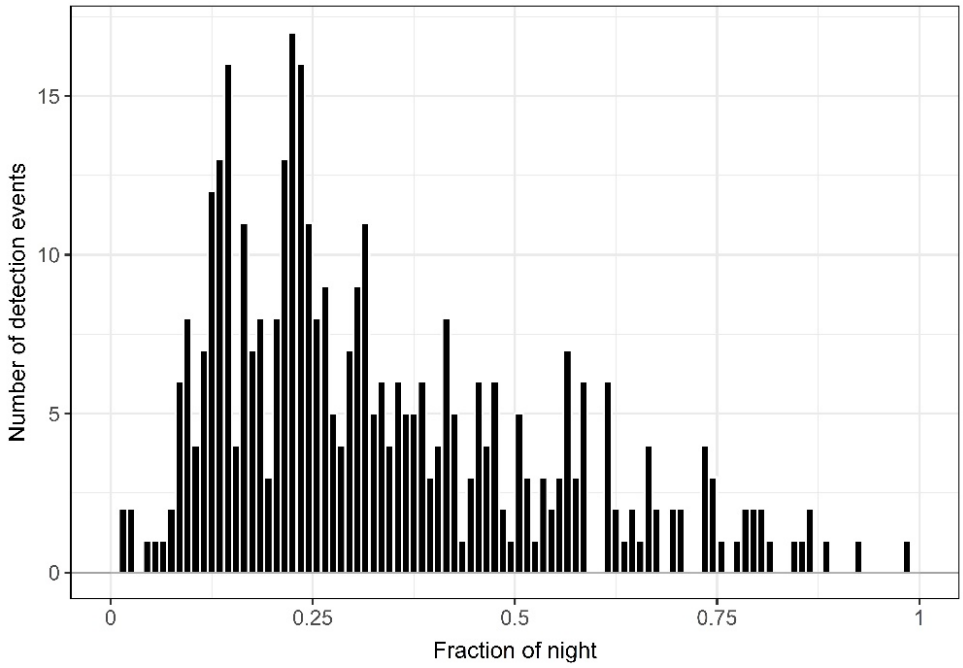

Figure 2. Distribution of visual detections of bats by time of night. To account for seasonal changes in night duration, the time of detection was standardized as a fraction of night and scaled from 0 (sunset) to 1 (sunrise).

Bats were detected throughout the four-month monitoring period (Figure 3), and linear regression demonstrated no evidence of a seasonal shift toward earlier or later activity during the night (slope = -1.17e-09, SE = 3.42e-09, $P = 0.733$). However, the rate of nightly bat detection (number of events per hour; adjusted for duration of night and sampling effort, including partially sampled nights) was highly variable among nights but evinced a seasonal pattern, with the rate decreasing (slope = -0.0005, SE = 0.0002, $P = 0.029$) from a mean of 0.11 events/hour (SE = 0.02) on survey night 1 (August 1) to 0.05 events/hour (SE = 0.02) on survey night 122 (November 30; Figure 4).

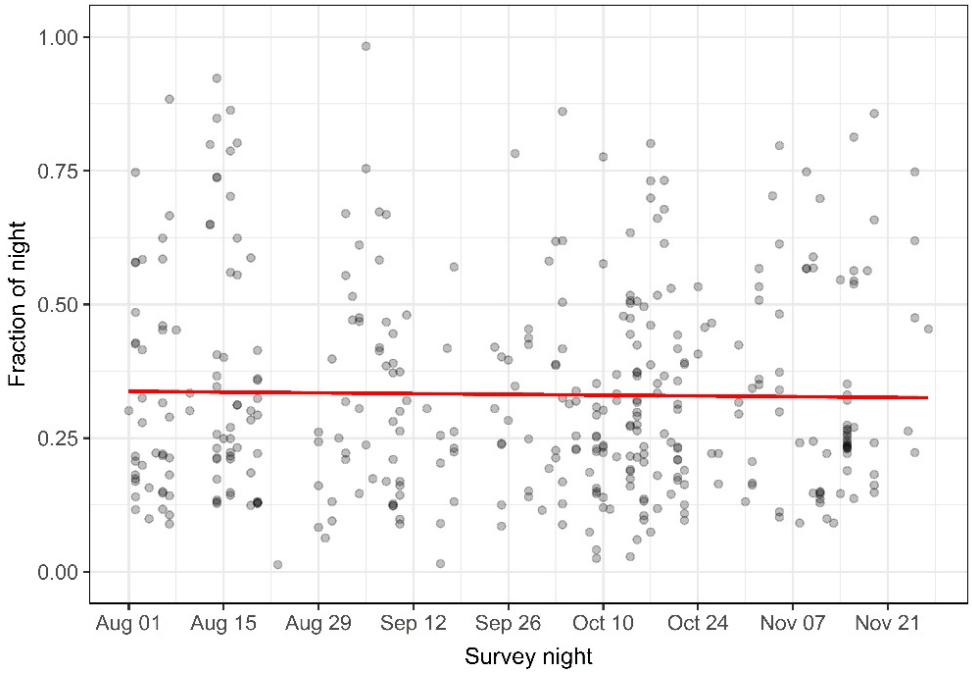

Figure 3. Detections (points) of bats by time of night over the four-month videographic monitoring period. To account for seasonal changes in night duration, the time of detection was standardized as a fraction of night and scaled from 0 (sunset) to 1 (sunrise). Situated below 0.5, the trendline of the mean values (red line) indicates a greater proportion of detections occurred in the first half of the night throughout the monitoring period.

The overall mean nightly detection rate for the entire videographic monitoring period was 0.08 events/hour (SD = 0.10, Q1 = 0.00, median = 0.04, Q3 = 0.13). Bat detection rates for each turbine were similar to the overall mean (Table 1, Figure 5) and not found to be significantly different from one another ($F[3, 402] = 0.885$, $P = 0.449$). Nightly detection rates demonstrated a weak but significant spatial correlation among turbines (all p-values <0.001), with pairwise Kendall's tau values ranging from 0.23 to 0.31 (Figure 6). The detection rate for all turbines combined demonstrated a weak positive relation with the rate on a previous night ($r = 0.18$), but the temporal pattern was not statistically significant to a lag of up to 12 nights (all p-values ≥ 0.05; Figure 7).

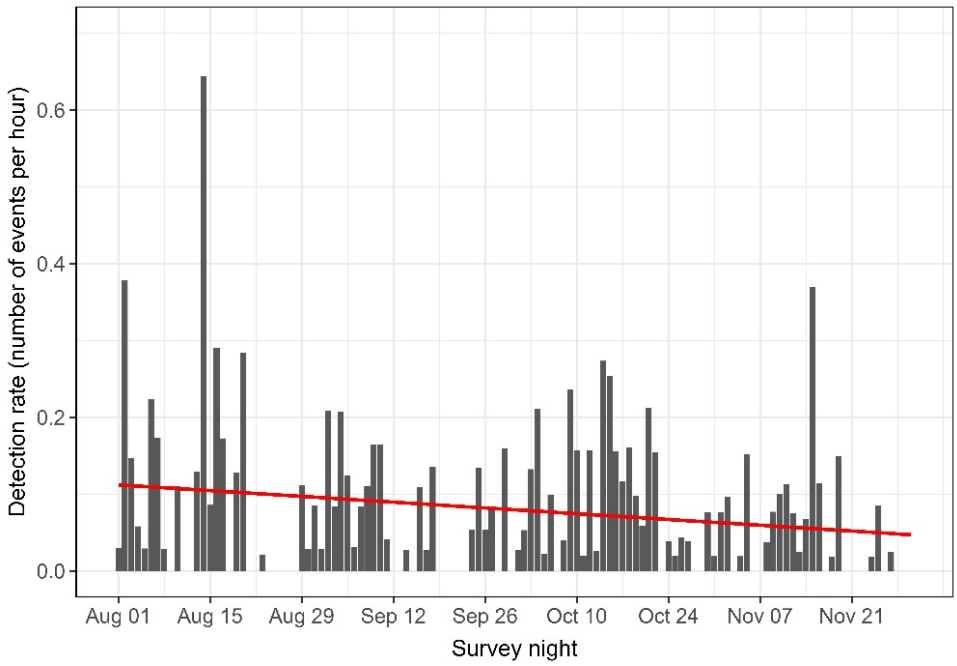

Figure 4. Detection rate of bats (number of events per hour per night) for all four turbines combined over the four-month videographic monitoring period. Detection rate is adjusted by survey effort (i.e., sample duration night interval and number of turbines monitored per night). The red line is a linear model of trend in detection rate over the monitoring period.

Table 1. Overall mean detection rate of bats by turbine (mean and SD). Detection rate was calculated as the nightly total of detection events at a turbine divided by the sample duration per night at the turbine. The combined mean is the overall average of the nightly detection rates for the four turbines over the four-month videographic monitoring period.

Turbine	Nightly mean (events/hour)	SD
2	0.07	0.10
4	0.07	0.13
5	0.09	0.14
7	0.07	0.11
combined mean	0.08	0.12

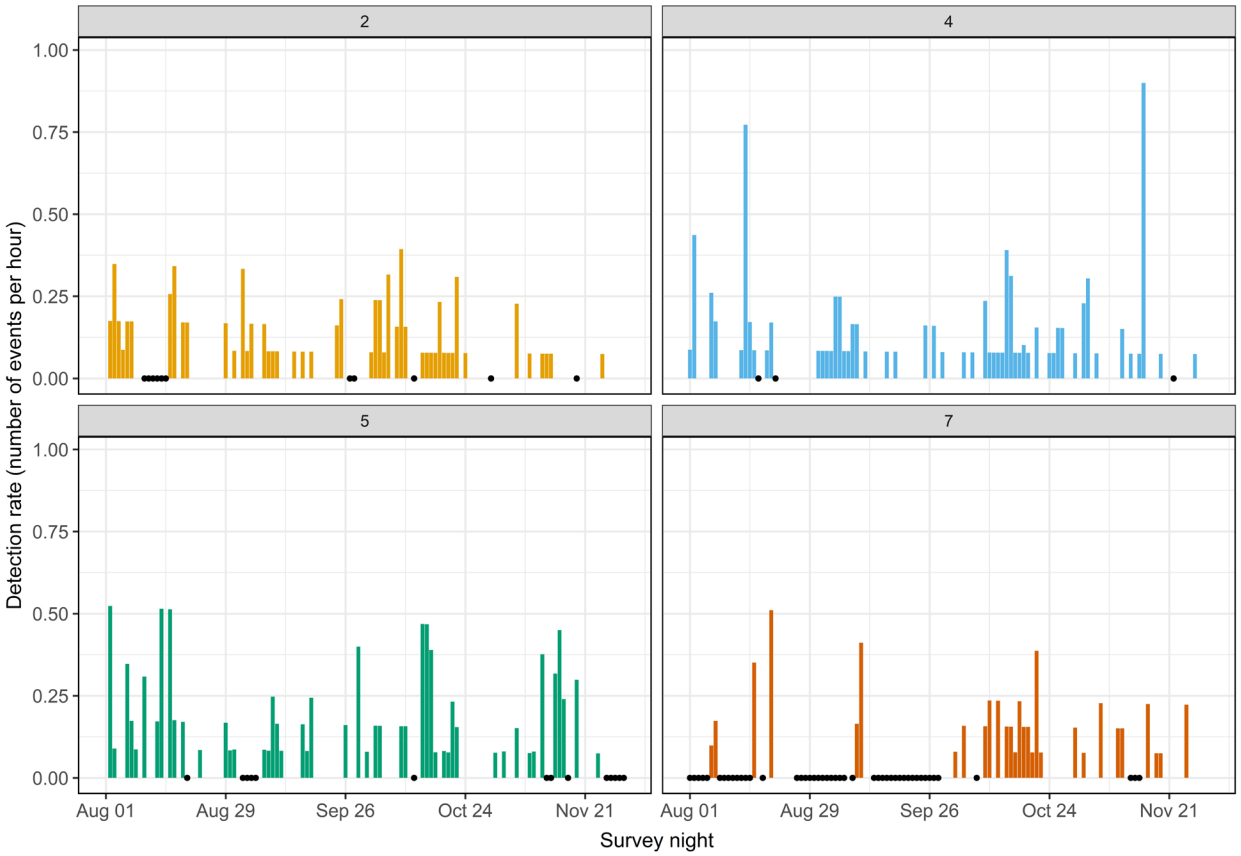

Figure 5. Detection rate of bats (number of events per hour per night) for each of four turbines (2, 4, 5, and 7) over the four-month videographic monitoring period. Detection rates are adjusted by survey effort (i.e., sample duration within night interval). Nights with no samples are indicated with a black point.

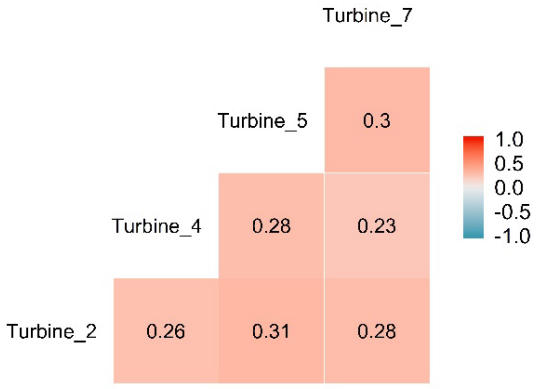

Figure 6. Spatial pairwise correlation of nightly detection rates between turbines. The p-values for all Kendall's rank correlation tau values are <0.001.

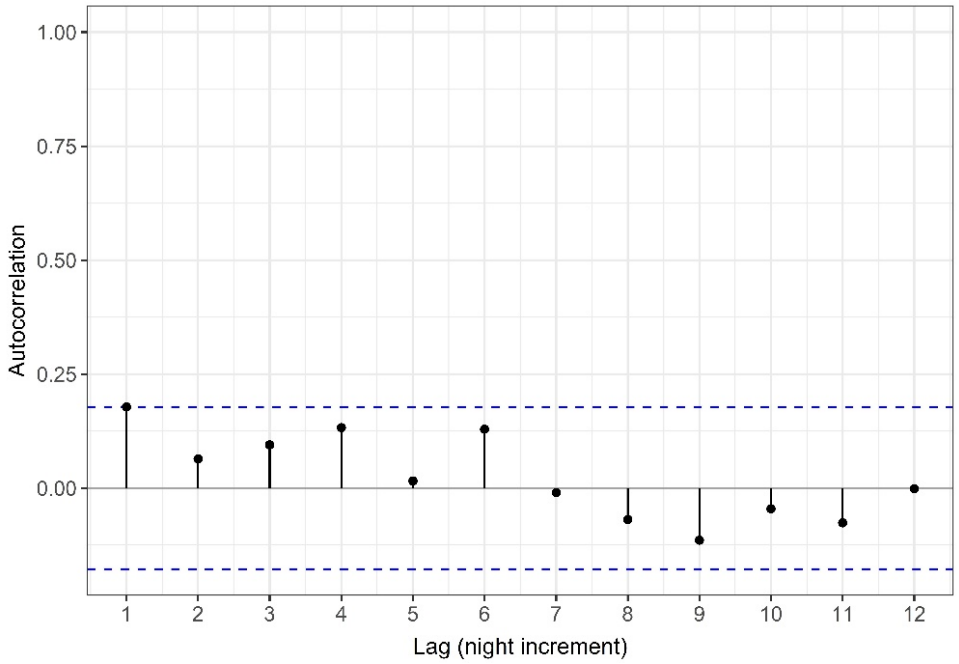

Figure 7. Temporal autocorrelation in the detection rate of bats (number of events per hour per night) for a series of lag increments up to 12 nights for all turbines combined over the four-month videographic monitoring period. Dashed lines indicate the threshold for statistical significance given sample size.

Almost all (n = 362; 94%) bat detections involved single bats within the 1-minute period used to quantify each event. Multiple bats seen concurrently were observed infrequently, with two bats (n = 22) observed during 6% of detection events, and no greater number noted at any time with any certainty. Most (n = 14) observations of two bats involved individuals not directly interacting, and bats were only rarely seen chasing (n = 5) or closely following each other (n = 3). All observations of bats engaged in chasing occurred when the individuals were in proximity (approx. <15 m) to the turbine nacelle.

The duration of individual bat detection events (in part determined by the limited field-of-view) averaged 23.5 sec per event. However, 11% (n = 41) of the events lasted 60 sec or more, with 4% (n = 14) of events lasting ≥120 sec, and one event was sustained for at least 211 sec (min = 0.5, Q1 = 3.8, median = 9.0, Q3 = 28.3, max = 211.2). On a per-turbine basis, the cumulative duration of nightly detection events averaged 50.1 sec (min = 0.6, Q1 = 7.1, median = 20.9, Q3 = 56.9, max = 804.2; Figure 8), with the maximum duration (totaling 13.4 minutes) comprised of a series of 12 distinct events (occurring on November 15 at turbine 4). The duration of detection events appears to moderately decline over time; however, linear regression demonstrated no evidence of a seasonal shift toward shorter or longer duration episodes of bat activity (slope = -0.016, SE = 0.012, $P = 0.187$) during the four-month period of monitoring (Figure 9). Although the individual and cumulative duration of detection events on some nights sometimes lasted several minutes, bats generally did not appear to be spending much time in the rotor-swept zone imaged by video. The duration of all detection events totaled to 150 minutes (9,015 sec) and made up only 0.05% of the total period of videographic

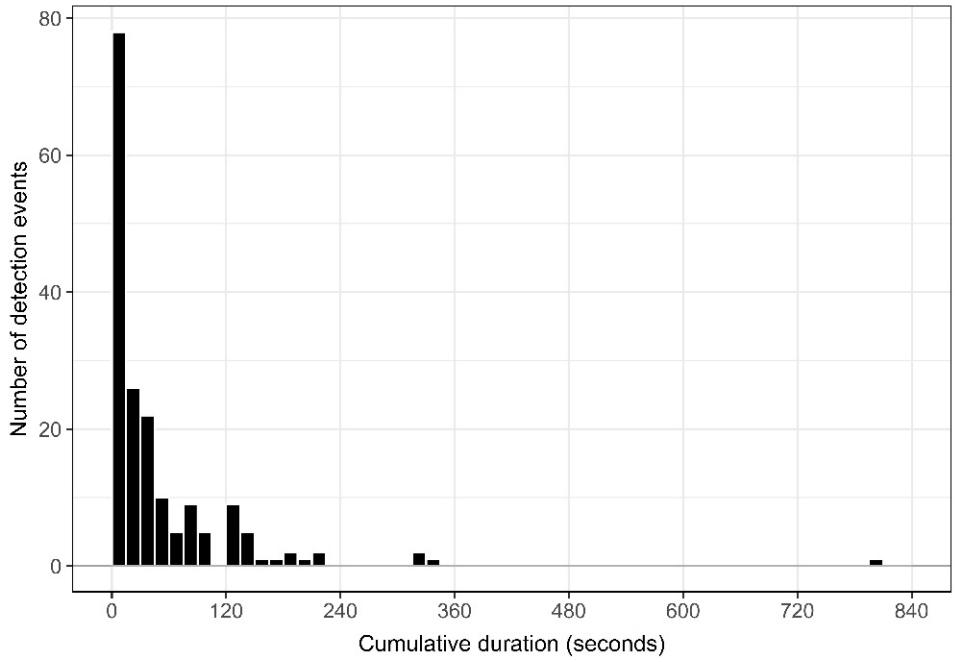

Figure 8. Distribution of the cumulative duration (seconds) of detection events on a nightly and per-turbine basis over the four-month monitoring period.

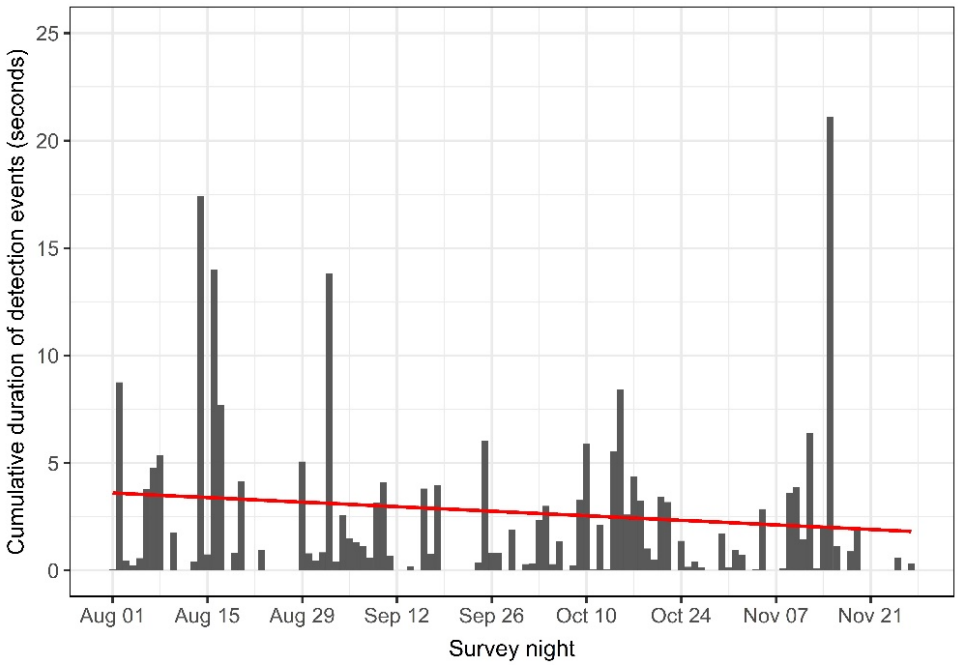

Figure 9. Cumulative duration (seconds) of detection events of bats on a nightly and per-turbine basis over the four-month monitoring period. The red line is a linear model of trend in event duration over the monitoring period.

monitoring (2.5 hours of 5,066 total hours). The time difference between consecutive detection events within a night averaged 80.4 minutes (min = 1.1, Q1 = 12.8, median = 49.0, Q3 = 101.2, max = 481.5; Figure 10). Most detection events consisted of a bat making a single pass through the field of view (57%; n = 220). Repeated passes (which together compose individual detection events when occurring <1 minute apart) were seen less frequently (2–4 passes [34%; n = 122], 5–10 passes [10%; n = 38], and 11–15 passes [1%; n = 4]).

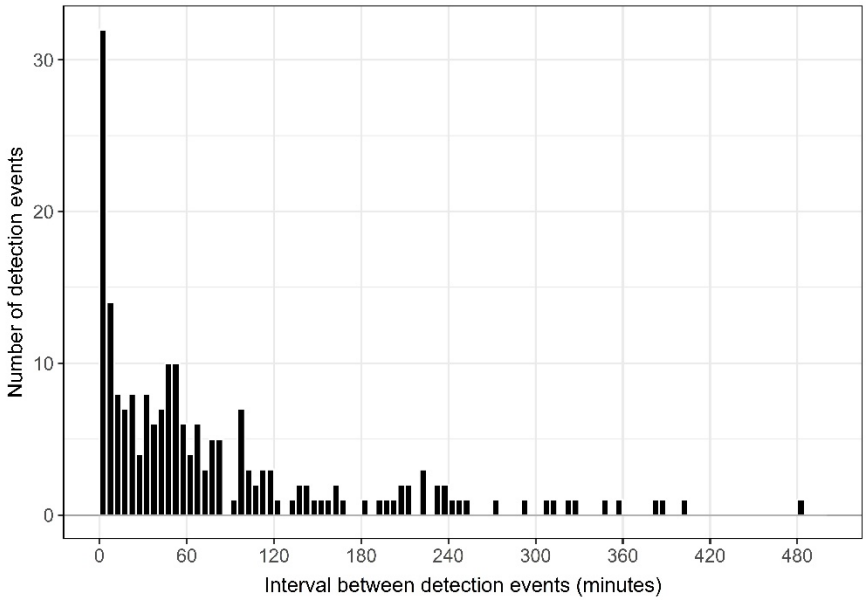

Figure 10. Distribution of the time interval (minutes) between consecutive detections of bats within a night combined for all turbines over the four-month monitoring period.

The largest proportion of bat detections involved erratic flight (80%; n = 306) suggestive of active foraging behavior in the immediate area of the turbine (i.e., within the video field-of-view; Table 2; Figure 11). Curved flight trajectories that may have involved either an approach towards or avoidance of the turbine were seen in 14% (n = 55) of events. Observations of straight flight paths indicative of a "fly-by" and little time spent near a turbine were observed in 6% (n = 23) of detections. Some of the observed curved and straight trajectories may simply consist of the less erratic parts of flight by bats otherwise engaged in foraging.

Table 2. Number and proportion of detection events by flight path type relative to bat proximity to nacelle (near = <15 m, far = ≥15 m).

Flight type	Near	Far
straight	13 (3%)	10 (3%)
curved	30 (8%)	25 (7%)
erratic	190 (49%)	116 (30%)
Total	233 (61%)	151 (39%)

Figure 11. Thermal video frame of a Hawaiian hoary bat at nacelle height (80 m) and within approximately 15 m of the nacelle (green dashed line), a distance within which vocalizing bats are likely to be recorded by acoustic detectors.

Most bat detection events (61%; n = 233) involved individuals that flew to within an estimated 15 m of the turbine nacelle. Comparatively, this 15-m radius area around the nacelle composed about a third of the video camera field-of-view; therefore, bats detected on video seemed to have closely approached the nacelle and upper monopole more often than not. Erratic flight paths were the most prevalent flight type observed, with bats repeatedly approaching and circling the nacelle in most cases. However, a Fisher's exact test did not demonstrate a significant relation ($P = 0.513$) between the number of events by flight path type as a function of bat proximity to turbine nacelle. Observations of displacement of bats or near-strikes by spinning turbine blades were seen in only two instances (0.5%). Direct strikes of bats by turbine blades were not observed.

Bats were most frequently detected at relatively low wind speeds (as measured at the turbine nacelle at 10-minute intervals; Figure 12). Wind speeds up to 3.4, 5.4, and 8.5 m/sec corresponded to 50%, 70%, and 90% of cumulative bat detection events, respectively, and

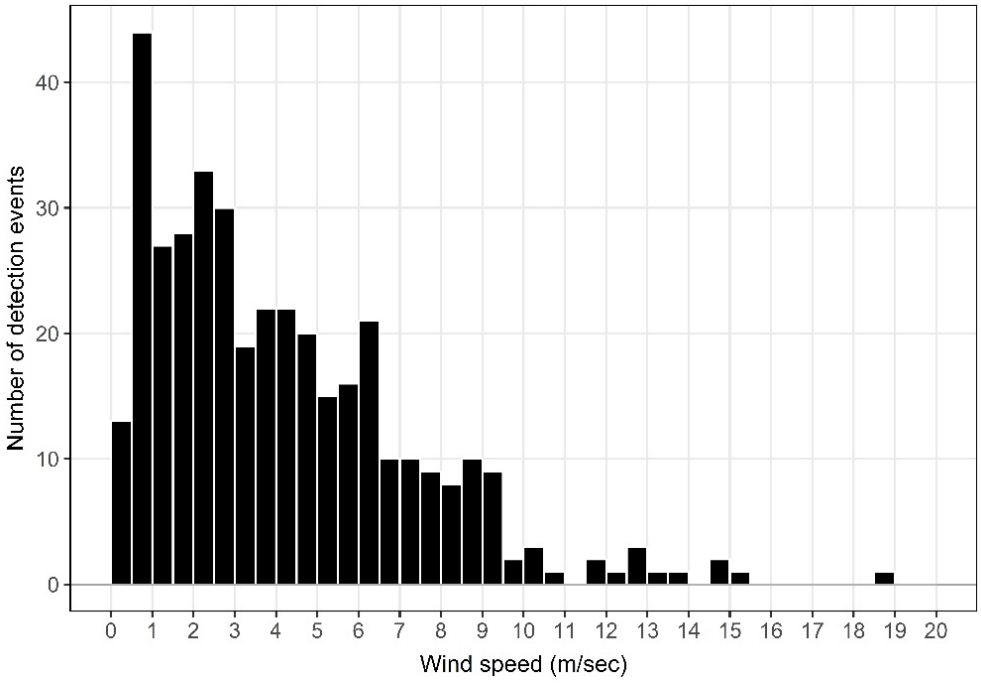

Figure 12. Distribution of bat detection events relative to wind speed (m/sec) measured at the turbine nacelle at 10-minute intervals over the four-month monitoring period.

10% of total detection events occurred at wind speeds between 8.5 m/sec and the maximum observed value of 18.9 m/sec (Table 3). A two-sample Kolmogorov–Smirnov (KS) test comparing wind speed during bat detection events to "ambient" nighttime conditions (both recorded at turbine nacelles) confirmed that the cumulative distributions were significantly different (KS test statistic D = 0.352, $P < 0.0001$; Figure 13). The KS test statistic D, defined as the maximum value of the absolute difference between the two cumulative distribution functions, was located at a wind speed value of 6.6 m/sec, corresponding to approximately 81% of cumulative bat detection events.

Table 3. Distribution of wind speed (m/sec) during bat detection events relative to randomly selected "ambient" nighttime conditions.

Samples	Mean	Median	70%	75%	80%	85%	90%	95%	100%
bat detection events	4.1	3.4	5.4	6.0	6.4	7.4	8.5	9.4	18.9
ambient nighttime	7.1	7.0	9.8	10.5	11.1	12.2	13.0	14.8	22.0

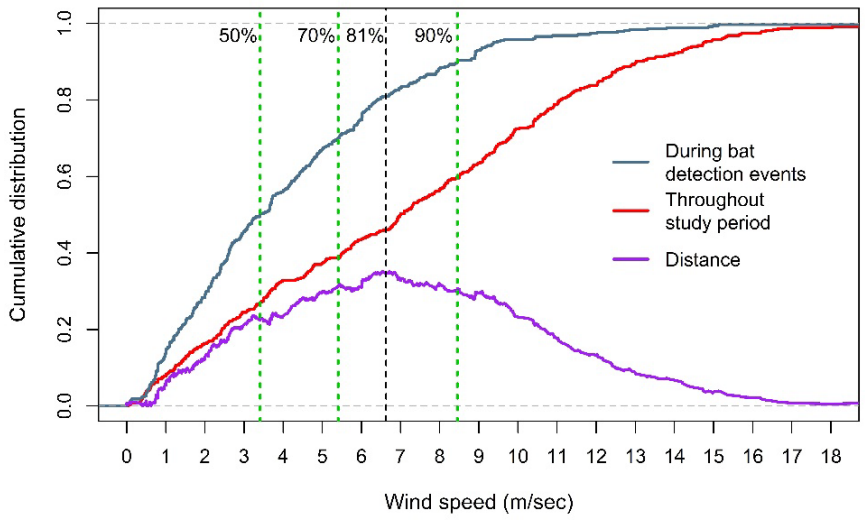

Figure 13. Cumulative distribution of wind speed (m/sec) during bat detection events relative to randomly selected "ambient" nighttime conditions recorded throughout the four-month monitoring period. A two-sample Kolmogorov–Smirnov (KS) test confirmed that the cumulative distributions were significantly different (KS test statistic D = 0.352, $P < 0.0001$). The KS test statistic D, defined as the maximum value of the absolute difference between the two cumulative distributions ("distance"), was located at a wind speed value of 6.6 m/sec, corresponding to approximately 81% of cumulative bat detection events (vertical dashed black line). Wind speeds for a range of cumulative distribution intervals (50%, 70%, and 90%) are shown with vertical dashed green lines.

There were relatively few bat detection events during periods when the turbine blades were in motion (Table 4, Figure 14). Bat observations during which there was no turbine rotation composed 81.5% (n = 313) of total events. A further 10.2% (n = 39) of events were observed at turbine rotor speeds of 0.1 to 0.5 rpm, with the remaining 8.3% (n = 32) at rpm values >0.5. However, of the 32 events that occurred when the turbine was moving >0.5 rpm, 8 events ensued when wind speeds were below the curtailment "cut-in" threshold (i.e., the wind speed at which the turbine begins to rotate and generate power; ≤6.9 m/sec for the period of August to October and ≤5.0 m/sec in November).

Table 4. Turbine rotations per minute (rpm) during bat detection events (number per rpm category) and proportion (percent).

Rpm	Number of events	Proportion
0	313	81.5%
>0–0.5	39	10.2%
>0.5–1.0	2	0.5%
>1.0–5.0	1	0.3%
>5.0–10.0	10	2.6%
>10.0–16.3 (max.)	19	4.9%

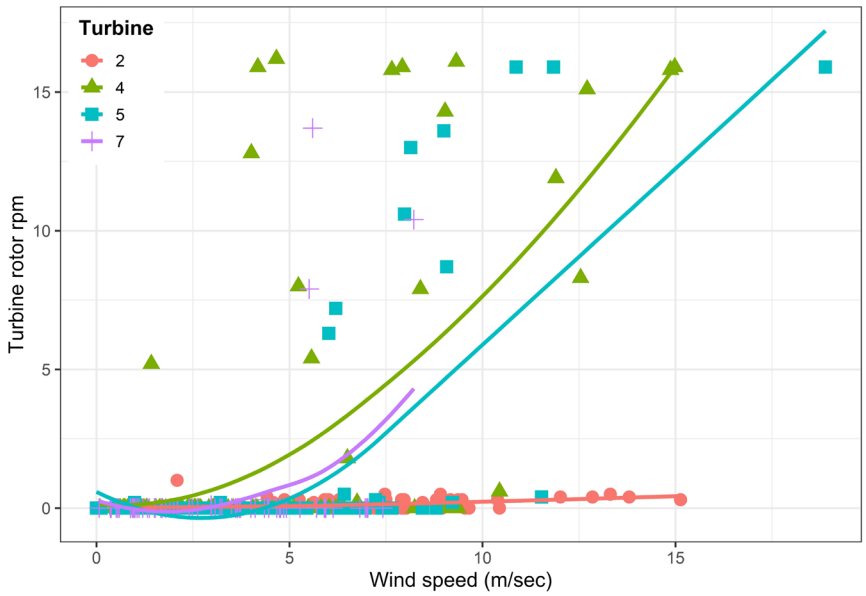

Figure 14. Turbine rotor rotations per minute (rpm) relative to wind speed (m/sec) during bat detection events over the four-month monitoring period. Locally estimated scatterplot smoothing (loess) curves are fit separately for turbines. Wind speed values are specific to the nearest 10-minute interval record. Turbine 2 was not operational, and rpm remained at or near zero until November 20 (10 nights before the end of monitoring).

Nightly bat detection rates for the four-month period of monitoring were negatively correlated with total daily precipitation (Kendall's rank correlation tau = -0.24, $P = 0.0009$). In addition, there were six periods lasting one or more nights with relatively high total daily precipitation (>1 cm) that corresponded with no bat detections or low detection rates (less than the nightly mean of 0.08 events per hour; Appendix I). These periods were associated with the passage of Hurricane Hector (August 9), Hurricane Lane (August 23–26), Tropical Storm Olivia (September 12–13), and strong low pressure systems (September 24–27, October 6–7, October 12) (National Weather Service Monthly Precipitation Summary, www.weather.gov/hfo/hydro_summary, accessed June 6, 2019).

Visual (Thermal Video) Bat Detections—Generalized Linear Mixed Model Analysis

The top-ranked GLMMs consistently included distribution types GP and CMP, indicating that underdispersion was effectively addressed in the final model selection. The weights of the top four models summed to 0.91, with only an additional weight of 0.06 gained from the fifth- and sixth-ranked models combined (Table 5). These models largely demonstrated similar combinations of variables (Table 6; summarized in Appendix II). All top models included either "wind-mean" or "rpm", and each of the models also included either "rpm-starts" or "wind-sd" (neither pairs were included jointly because of their high correlation). Diagnostics demonstrated that the final regression models met assumptions of uniformity and did not exhibit zero inflation (Appendix III), with underdispersion addressed in GP and CMP models. Data used in models are available at https://doi.org/10.5066/P937H9LQ (Gorresen 2020).

Table 5. Generalized linear mixed models ranked by model fit. "Type" refers to model distribution type: generalized Poisson (GP) or Conway-Maxwell-Poisson (CMP). "log L" refers to the estimate of the log-likelihood and "DF" refers to model degrees of freedom.

Model	Type	Predictor variables			log L	AICc	Δlog L	ΔAICc	DF	Weight
1	CMP	rpm	wind-sd	precip	-470.5	955.4	38.8	0.0	7	0.43
2	CMP	rpm	wind-sd		-472.2	956.6	37.2	1.2	6	0.23
3	GP	wind-mean	rpm-starts		-472.7	957.7	36.6	2.3	6	0.14
4	GP	wind-mean	rpm-starts	precip	-471.9	958.1	37.5	2.7	7	0.11
5	GP	wind-mean	wind-sd		-473.8	959.9	35.5	4.5	6	0.04
6	GP	wind-mean	wind-sd	precip	-473.5	961.3	35.8	6.0	7	0.02
7	GP	rpm	precip		-475.2	962.6	34.2	7.2	6	0.01
8	GP	rpm	rpm-starts	precip	-475.2	964.6	34.2	9.2	7	<0.01
9	GP	rpm			-477.9	965.9	31.5	10.6	5	<0.01
10	GP	rpm	rpm-starts		-477.8	967.7	31.6	12.3	6	<0.01
11	GP	wind-mean	precip		-480.0	972.2	29.4	16.8	6	<0.01
12	GP	wind-mean			-481.3	972.7	28.1	17.4	5	<0.01
13	GP	precip			-502.8	1015.7	6.6	60.4	5	<0.01
14	GP	rpm-starts	precip		-502.0	1016.3	7.3	60.9	6	<0.01
15	GP	wind-sd	precip		-502.7	1017.6	6.7	62.2	6	<0.01
16	GP	null			-509.4	1026.8	0.0	71.5	4	<0.01
17	GP	rpm-starts			-508.6	1027.4	0.8	72.0	5	<0.01
18	GP	wind-sd			-509.4	1028.9	0.0	73.5	5	<0.01

Table 6. Standardized model estimates and associated measures from the six top-ranked GLMMs (combined weight = 0.97) predicting the effect of weather and turbine operation variables on the number of nightly bat detections events. Number of observations for all models = 412.

Model	Parameter	Estimate	SE	z value	p-value	Variance
1	Random effect					
	night (Intercept)					0.38
	turbine					0.21
	Conditional model					
	(Intercept)	-3.22	± 0.26	-12.47	<0.0001	
	rpm	-1.13	± 0.14	-8.26	<0.0001	
	wind-sd	0.31	± 0.09	3.29	0.0010	
	precip	-0.27	± 0.17	-1.62	0.1055	
2	Random effect					
	night (Intercept)					0.38
	turbine					0.23
	Conditional model					
	(Intercept)	-3.19	± 0.27	-11.91	<0.0001	
	rpm	-1.18	± 0.13	-8.80	<0.0001	
	wind-sd	0.33	± 0.09	3.60	0.0003	
3	Random effect					
	night (Intercept)					0.42
	turbine					0.02
	Conditional model					
	(Intercept)	-3.17	± 0.14	-22.15	<0.0001	
	wind-mean	-1.08	± 0.13	-8.05	<0.0001	
	rpm-starts	0.40	± 0.09	4.23	<0.0001	
4	Random effect					
	night (Intercept)					0.41
	turbine					0.02
	Conditional model					
	(Intercept)	-3.19	± 0.14	-22.04	<0.0001	
	wind-mean	-1.04	± 0.14	-7.49	<0.0001	
	rpm-starts	0.39	± 0.09	4.12	<0.0001	
	precip	-0.21	± 0.18	-1.16	0.2450	
5	Random effect					
	night (Intercept)					0.42
	turbine					0.00
	Conditional model					
	(Intercept)	-3.15	± 0.13	-24.20	<0.0001	
	wind-mean	-1.09	± 0.14	-7.94	<0.0001	
	wind-sd	0.39	± 0.10	3.95	<0.0001	
6	Random effect					
	night (Intercept)					0.42
	turbine					0.00
	Conditional model					
	(Intercept)	-3.16	± 0.13	-23.97	<0.0001	
	wind-mean	-1.06	± 0.14	-7.335	<0.0001	
	wind-sd	0.37	± 0.10	3.675	0.0002	
	precip	-0.14	± 0.18	-0.743	0.4575	

Acoustic Bat Detections—Descriptive Analyses

Acoustic monitoring at the four turbines yielded 247 turbine-nights of viable recording, comprising 3,036 hours of sampling (including a 15-minute period before sunset and after sunrise; turbine 2 [767.0 hrs], turbine 4 [212.2 hrs], turbine 5 [1,446.7 hrs], turbine 7 [610 hrs]). During this period a total of 1,873 wav sound files with confirmed bat detections were acquired from the rear-facing (leeward) microphone. Detections pooled into groups that occurred within 1 minute of each other totaled to 244 discrete events. Bats were detected acoustically in 31% (n = 75) of the turbine-nights sampled. Acoustic bat detection data are available at https://doi.org/10.5066/P937H9LQ (Gorresen 2020) and are summarized in Appendix I and II.

Acoustic detections of bats at turbines occurred throughout the night, with the earliest detection occurring 25 minutes after sunset and the latest 18 minutes before sunrise. Detections exhibited a unimodal distribution and a median fraction of night time of detection equal to 0.28, corresponding to a peak about 3.3 hours after sunset (Q1 = 0.19, Q3 = 0.40, mean = 0.32 ± 0.18 SD; standardized as a fraction of night and scaled from 0 at sunset to 1 at sunrise; Figure 15). A Welch two-sample t-test (Delacre *et al.* 2017) of the bat observations produced by video and acoustic monitoring found no significant difference in the mean time of detection events between the two sampling methods (t = 1.0592, df = 558.37, $P = 0.290$).

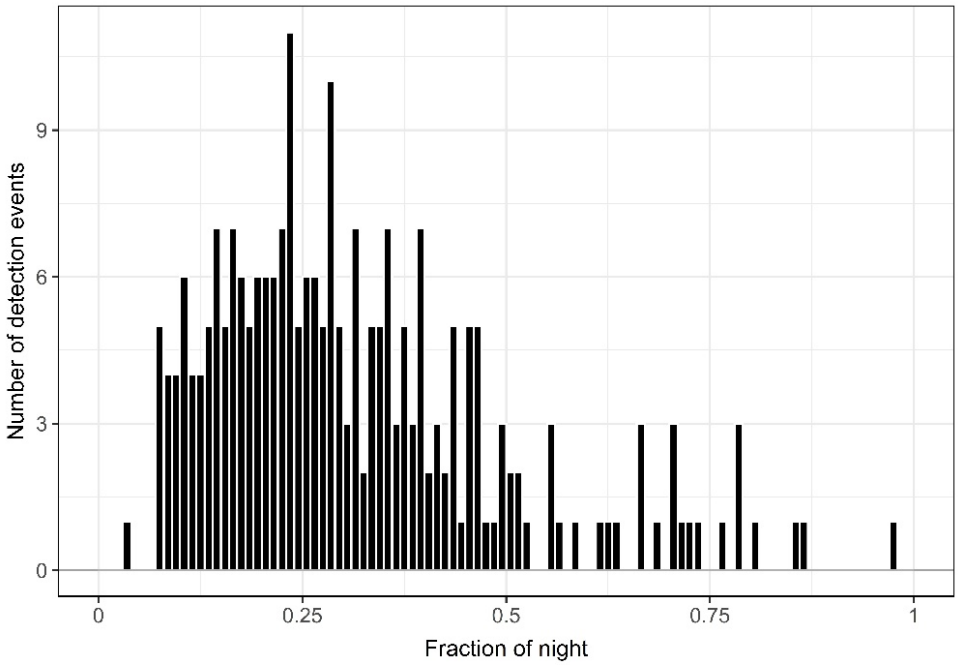

Figure 15. Distribution of acoustic detections of bats by time of night over the four-month monitoring period. To account for seasonal changes in night duration, the time of detection was standardized as a fraction of night and scaled from 0 (sunset) to 1 (sunrise).

The overall mean acoustic detection rate for which data were available was 0.08 events/hour (SD = 0.18; Q1 = 0.00, median = 0.00, Q3 = 0.08). Because the acoustic samples were largely concentrated on the earlier part of the four-month monitoring period (Figure 16), a direct comparison for all turbines combined with the rate obtained from videographic sampling was not possible. However, acoustic samples for turbine 5 were comparable in the span of the monitoring period that matched video samples, and a Welch two-sample t-test found no significant difference in the mean detection rate between the two sampling methods (t = 1.7011, df = 167.11, $P = 0.0978$). Extensive periods with missing acoustic data and uncertainty in the decay rate of microphone sensitivity did not permit a quantitative comparison of detection rates among turbines relative to time of year.

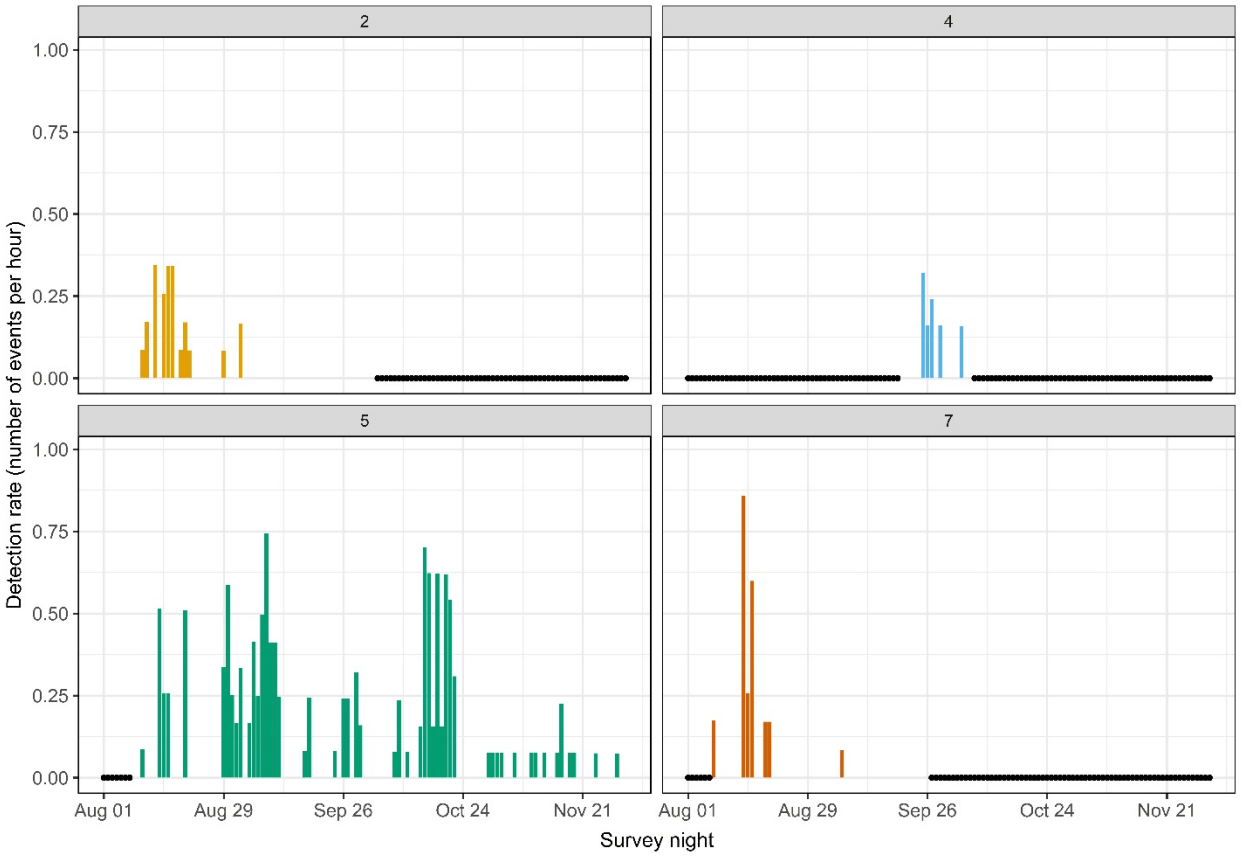

Figure 16. Detection rate of bats (number of events per hour per night) for each of four turbines (2, 4, 5, and 7) over the four-month acoustic monitoring period. Detection rates are adjusted by survey effort (i.e., sample duration within night interval). Nights with no samples are indicated with a black point.

The duration of individual acoustic bat detection events (in part determined by the range acoustic detectors are capable of sampling) averaged 23.2 sec per event. However, 7% (n = 17) of the events lasted 60 sec or more, of which 2% (n = 5) of events lasted ≥120 sec, and one event was sustained for 13.4 minutes (min = 3.0, Q1 = 3.0, median = 6.0, Q3 = 21.0, max

= 803.0 sec). On a per-turbine basis, the nightly cumulative duration of events averaged 76.0 sec (min = 3.0, Q1 = 6.0, median = 36.0, Q3 = 71.0, max = 1,232.0; Figure 17), with the maximum duration (totaling to 20.5 minutes) comprised of 14 individual events (occurring on September 25 at turbine 5). Although the cumulative duration of events appears to more than halve during the four-month period of monitoring, high variance precluded the detection by linear regression of a seasonal change in the duration of bat activity (slope = -0.0446, SE = 0.0329, *P* = 0.1805; Figure 18). As with the results inferred from visual (thermal video) monitoring, acoustic sampling indicated that bats generally do not appear to be spending much time in the rotor-swept zone. The duration of all detection events totaled to 94 minutes (5,650 sec) over the survey and made up only 0.05% of the total period of acoustic monitoring (1.6 hours of 3,036 total hours). Acoustic detections were infrequent and the time difference between consecutive events within a night averaged 65.4 minutes (min = 1.4, Q1 = 14.4, median = 38.8, Q3 = 74.7, max = 530.6; Figure 19). Most nightly detection events (57%; n = 44) at a turbine were comprised of 10 or fewer "bat passes" (i.e., distinct wav files). More numerous passes were recorded less frequently: >10 to 100 passes (40%; n = 31); >100 passes (3%; n = 2; Figure 20). Terminal-phase (feeding buzz) type calls were only noted in 3% (n = 7) of all events.

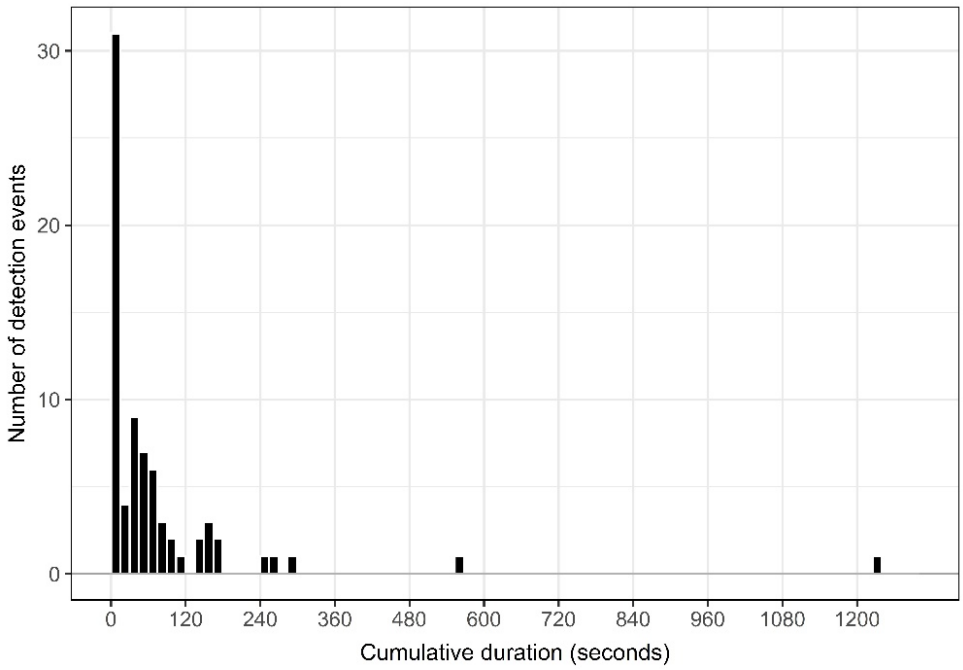

Figure 17. Distribution of the cumulative duration (seconds) of acoustic detection events on a nightly and per-turbine basis over the four-month monitoring period.

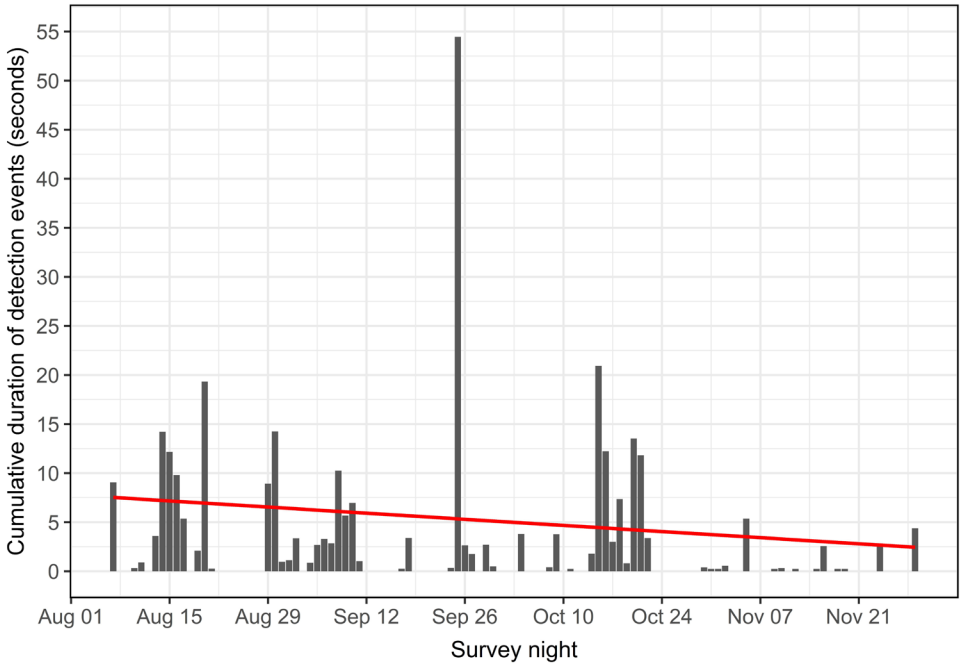

Figure 18. Cumulative duration (seconds) of acoustic detection events (adjusted for total nightly sampling duration for all turbines) over the four-month monitoring period. The red line is a linear model of trend in event duration.

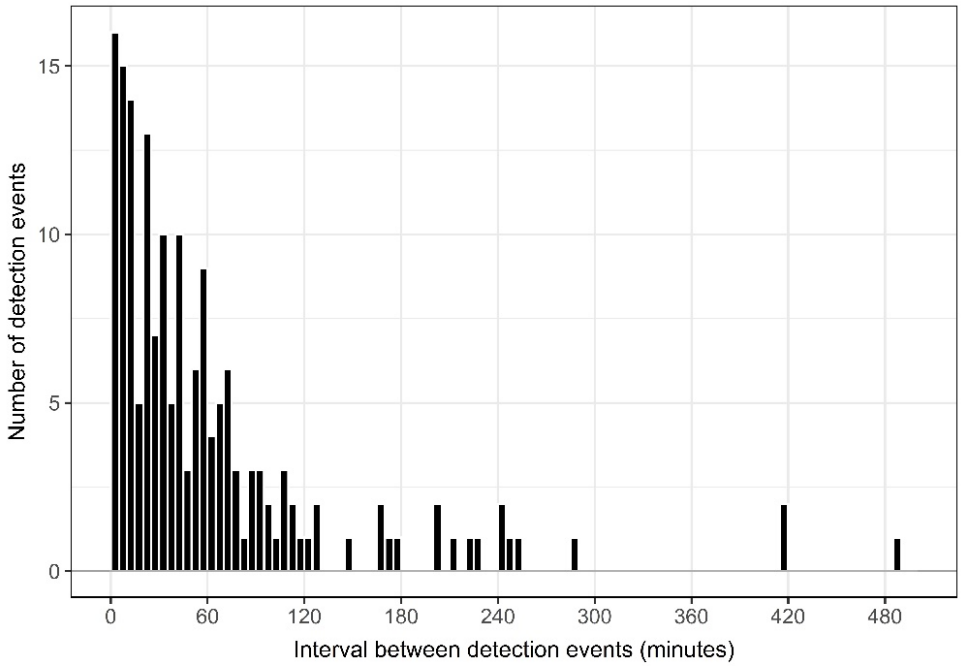

Figure 19. Distribution of the time interval (minutes) between consecutive acoustic detections of bats within a night over the four-month monitoring period.

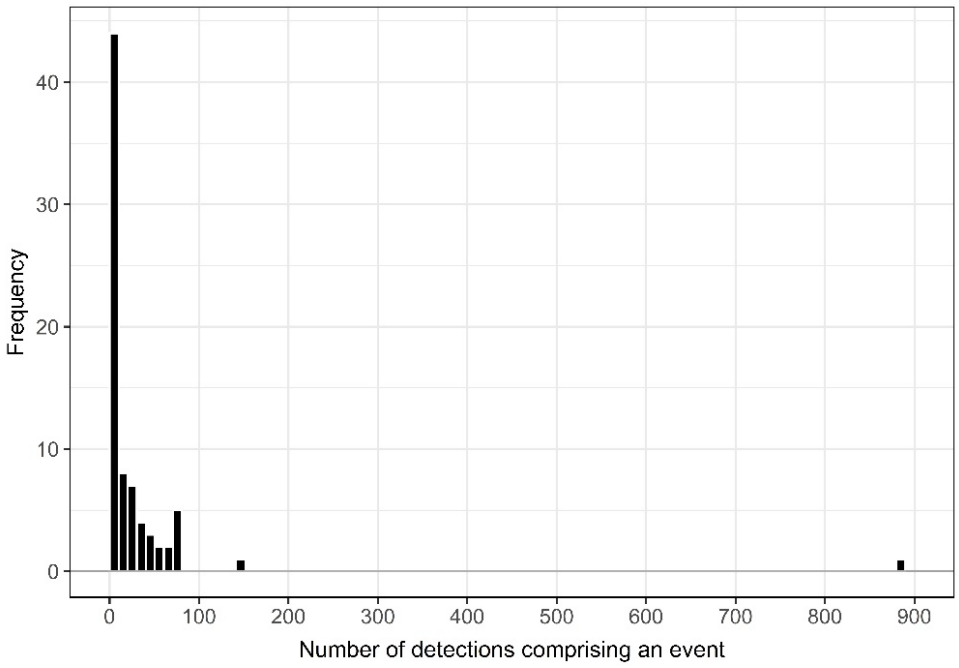

Figure 20. Distribution of the number of discrete detections (wav sound files measuring "bat passes") that comprised events over the four-month monitoring period.

The correspondence between acoustic and visual detection events at a turbine were examined at three scales: the entire night (averaging approximately 12 hours); a 2-hour period (i.e., an acoustic detection 1 hour before or after a visual detection); and a 10-minute period (i.e., an acoustic detection 5 minutes before or after a visual detection). A total of 187 turbine-nights was concurrently sampled both acoustically and visually. Of this subset, acoustic detections (regardless of whether it was also detected visually) composed 33% (n = 62) of the concurrently sampled turbine-nights (Table 7). Acoustic samples confirmed bat presence on 56% (= 45/81) of the turbine-nights for which bats were also detected visually with thermal cameras at some point during the night. Bats were not detected by either method during 48% (n = 89) of the concurrent sample.

Table 7. Proportion of concurrently sampled turbine-nights (n = 187) with bat detections.

Sample method	Nights bats detected
Both visual & acoustic	45 (24%)
Visual only	36 (19%)
Acoustic only	17 (9%)
Neither method	89 (48%)
Visual only plus both visual & acoustic	81 (43%)
Acoustic only plus both visual & acoustic	62 (33%)

At a finer temporal scale, there were a total of 294 visual detection events during the concurrently sampled period, of which 22% (n = 65) of acoustic detections occurred within a 2-hour window of a visual detection, and of these, a subset of 12% (n = 36) occurred within a 10-minute window. Conversely, a total of 229 visual detection events did not have an acoustic match within a 2-hour window, even though 65% (n = 149) of these involved a bat making a close approach to the nacelle (i.e., within approximately 15 m).

DISCUSSION

Our findings reveal new information about the potential effects of wind speed and turbine operation on the presence and behavior of Hawaiian hoary bats occurring on the coast of southwest Maui. We used complementary observation technologies (sound recordings and video imaging) over four months to document distinct seasonal and nightly patterns in the occurrence and activity rates of hoary bats at the Auwahi Wind Energy facility. Overall, the picture emerging from these results is that individual hoary bats from other parts of the island sporadically visit the wind facility, usually before midnight, dwell in the airspace near each turbine for a few seconds (probably searching for insect prey), and then move out of the area without returning for several nights. Bat activity patterns across the local landscape were likely affected by the presence of wind turbines, weather conditions, and possibly operational changes implemented as mitigation efforts. These findings offer unique perspective toward broadening our understanding of the behavioral reasons why bats might regularly approach wind turbines, gauging the efficacy of different monitoring and research technologies, and point to new possibilities for fatality reduction.

We observed bat activity at the Auwahi wind turbines from early August through late November of 2019. Although this timespan represents an intensive field and analysis effort, it only covered one-third of an annual cycle during a single year, so our conclusions are based on conditions that happened to occur at the study site during this period. Lacking additional longer-term, site-specific information, the following discussion assumes that the patterns we report are representative of typical bat visitation, weather conditions, and turbine operation at the site.

Although we detected a slight downward trend in bat visitation to the wind turbines from August through November of 2019, bat activity was consistently low and sporadic. This downward seasonal trend differs from more distinct patterns of hoary bat activity observed at wind facilities studied using comparable methods on nearby islands (Gorresen *et al.* 2015b) and on the U.S. mainland (Cryan *et al.* 2014). At a wind facility on the island of Oʻahu, bat visitation to turbines increased during a six-month study period spanning from mid-May through mid-November of 2013, peaking in November (Gorresen *et al.* 2015b). We are not aware of other comparable data sets relevant to Hawaiian hoary bats. On the U.S. mainland and Canada, hoary bat fatality and video activity at wind turbines generally begins increasing in mid-June, tends to peak in September, then decreases by October and November (Arnett and Baerwald 2013, Cryan *et al.* 2014).

The question of whether bat activity and presumably collision risk in Hawaiʻi is seasonally consistent or peaks during certain times of year remains unanswered. The hypothesis that seasonal peaks in hoary bat fatalities at turbines on the mainland have more to do with migration than other factors (Cryan and Barclay 2009), and thus the non-migratory Hawaiian

hoary bat would be less susceptible, is yet untested. The possibility remains that factors other than migration, such as feeding or mating strategies that trigger bat investigation of tall landscape structures, primarily drive the seasonal peaks of bat fatalities observed elsewhere (Cryan and Barclay 2009, Cryan *et al.* 2014). Considering our results and available information, seasonal peaks in bat activity and fatality rates at wind turbines may occur in Hawai'i too, yet to our knowledge relevant year-long observations of occurrence combined with fatality monitoring have not been made at a sufficient number of wind energy facilities within the range of the Hawaiian hoary bat to discern whether or not a distinct and consistent seasonal peak occurs. Clearly establishing the existence and temporal consistency of seasonal peaks in bat activity at wind turbines has clear implications toward design and implementation of operational fatality reduction strategies.

We observed both similarities and differences in the nightly activity patterns of bats at the Auwahi Wind Energy facility compared to those uncovered using similar methods at turbines on O'ahu and the U.S. mainland. The bat detection rate at the Auwahi Wind Energy facility, measuring in the hundredths of bat detections per hour over the approximately 5,000 hours of video observation, was much lower than that observed during a comparable video-based study on O'ahu. The detection rate at the Auwahi Wind Energy facility was about an order of magnitude lower than was observed at turbines in an upland forest site on O'ahu, where bat detections numbered in the tenths (0.88) per hour over almost 4,000 hours of video, and which also included additional months with low bat activity (mid-May through July; Gorresen *et al.* 2015b). Similar to patterns observed on the U.S. mainland, hoary bat activity around the turbines at the Auwahi Wind Energy facility mostly occurred during the first half of the night, although bats were sometimes active in the hours before dawn (Cryan *et al.* 2014). This nightly activity pattern of a single activity peak more than an hour after sunset yet before midnight differs from that documented over six months at the upland forest turbines on O'ahu in 2013, where detections showed not only an earlier primary peak immediately after sunset, but also a smaller secondary peak in the hours just before dawn (Gorresen *et al.* 2015b).

Possible explanations for the single, lower, and slightly later nightly activity peak of Hawaiian hoary bats at the Auwahi Wind Energy facility include individuals having to commute to the site after emerging from roosts at sunset in nearby habitats (likely forests), and environmental conditions that potentially draw bats to turbines from the broader landscape being more likely to occur at that time. On O'ahu, the peaks of highest bat detections coincided with sunset and sunrise, indicating that bats were likely to visit turbines immediately after emerging from or returning to roosts in the surrounding forest. The lack of such crepuscular activity peaks at the Auwahi Wind Energy facility lead us to believe that bats visiting the turbines there do not roost during the daytime at or near the site, but instead reach the turbines by flying from more distant locations—probably tree roosts in denser forest stands, the closest of which are about 7 km away. The pattern also indicates bats do not regularly visit the Auwahi Wind Energy facility turbines in the hours before sunrise. The possibility of early nighttime environmental conditions that might draw bats to turbines are discussed below.

In addition to generally observing fewer visits by bats, a delayed post-sunset activity peak, and the lack of a pre-dawn activity peak, another notable pattern in the nightly activity of bats at the Auwahi Wind Energy facility was their sporadic occurrence at the wind facility from night to night. Our results indicate that when bats visit the wind facility, they tend to dwell around the turbines for slightly longer on a per-visit basis than was observed in upland forest at the wind facility on O'ahu. The duration of individual bat detection events at the Auwahi Wind Energy

facility averaged 23.5 sec and were about six times longer than the duration of detections recorded at the O'ahu forest site, which averaged 4.0 sec per event (Gorresen *et al.* 2015b). However, the cumulative amount of time bats spent around a turbine on a nightly basis was remarkably similar between the two studies, with cumulative times totaling about 40 and 50 sec per turbine per night at the site on O'ahu and at the Auwahi Wind Energy facility, respectively (Gorresen *et al.* 2015b). These findings show that although Hawaiian hoary bats visit the Auwahi Wind Energy facility less frequently, their longer nightly visits could result in individuals spending an equivalent amount of time per night around turbines as at the forested site on O'ahu. However, patterns in the spacing of bat detections at the Auwahi Wind Energy facility within and among nights indicates potential differences in the way bats perceive and interact with wind turbines there compared to other sites.

Two notable patterns we observed at the Auwahi Wind Energy facility were the correlation of bat detections among turbines and the relatively long and unpredictable time periods between consecutive detection events, both within and among nights. Within a given night, visiting bats tended to dwell at the site and were likely to visit many of the turbines before leaving. When they did leave the site, an average of 1 hour 20 minutes elapsed before another bat was detected. On a night-to-night basis, bat occurrence was sporadic and unpredictable. That is, a Hawaiian hoary bat using the wind facility on a given night may not be strongly predictive of a bat occurring there again on subsequent nights or be strongly influenced by cyclic or other night-to-night patterns caused by short-term factors or predictable environmental conditions (at least within the 12-night analysis window we examined). The relatively infrequent, unpredictable, and lingering observations of Hawaiian hoary bats detected at the Auwahi Wind Energy facility could be attributable to certain wide-ranging individuals sporadically but repeatedly commuting to the site from distant roosting areas, multiple wide-ranging individuals haphazardly encountering the turbines during more randomly directed landscape movements, or some combination of these scenarios. Activity patterns of Hawaiian hoary bats observed in forested habitats on O'ahu led to speculation that those individual bats were familiar with turbines interspersed among their roosting and foraging grounds, and the resources (e.g., prey, mates, etc.) available at those structures (Gorresen *et al.* 2015b). It remains to be determined whether bats visiting turbines at the Auwahi Wind Energy facility are naïve to the resources sought at the turbines or if they become familiar and less risk-prone as experienced individuals.

The relatively longer periods of observation per bat visit at the Auwahi Wind Energy facility gave us better opportunities than in previous studies to determine why those hoary bats might have been flying in the airspace near the turbines. The duration of all detection events in this study totaled only 2.5 hours and made up only 0.05% of the entire period of video monitoring. This cumulative total was less than in the study at turbines in upland forest on O'ahu, where bat video observations totaled about 3.8 hours and represented 0.1% of video analyzed (Gorresen *et al.* 2015b). As discussed above, despite less frequent detections at the Auwahi Wind Energy facility, the longer duration of events there resulted in the cumulative period of bat detections per turbine per night being similar between the two studies. However, bats at the Auwahi Wind Energy facility were observed for proportionally longer periods per detection event, giving us more opportunities to accurately discern behaviors during these typically brief encounters.

Eight out of ten of the observations of Hawaiian hoary bats around wind turbines at the Auwahi Wind Energy facility involved erratic flight indicative of bats engaged in foraging behavior. Only a small proportion of events involved straight, directed flight past the turbines, suggestive of

bats quickly transiting the rotor-swept airspace. The proportion of events involving foraging-like flight at the Auwahi Wind Energy facility was approximately double that documented during the study on O'ahu, where turbines were situated in upland forest, and bat activity correlated to insect activity (Gorresen *et al.* 2015b). A 2017 videographic survey of upland habitats on O'ahu (including the wind facility mentioned previously) also showed that most bat detection events involved single passes involving straight and directed flight, suggestive of samples obtained from bats moving within frequently traversed home ranges (Gorresen *et al.* 2018). The bats at the Auwahi Wind Energy facility may have been concentrating their flight and associated search for food disproportionately more on the wind turbines than on surrounding habitats, whereas those observed on O'ahu may have been primarily moving through the habitats with ample feeding opportunities surrounding the turbines and thus spending proportionally less time focusing on the turbines. Overall, our observations indicate bats travel from distant roost sites to the remote but potentially focal foraging area around the Auwahi Wind Energy facility turbines, search promising habitat features (including the turbines themselves) for insect prey, then leave and only infrequently return during the same or subsequent nights. In contrast, the proportionally lower incidence of foraging-like behavior observed around turbines in forested uplands of O'ahu might have been attributable to those turbines being situated amidst more favorable alternative foraging prospects.

Regardless of why bats entered the airspace around wind turbines at the Auwahi Wind Energy facility, more than half of the detection events involved individuals flying within an estimated 15 m of the turbine nacelle. This regular and consistently observed close-approach behavior, combined with relatively few observations of bats being displaced by moving blades and no observation of strikes, indicates that the presence of Hawaiian hoary bats in the rotor-swept zone of a turbine may not be directly proportional to their risk of being injured, particularly when presence is considered independent of wind speed. Systematic ground-based carcass searches resulted in no documented bat fatalities at the four turbines during the four-month monitoring period (Tetra Tech 2019).

The activity of bats is generally believed to decrease with increasing wind speed (Weller and Baldwin 2012, Korner-Nievergelt *et al.* 2013), as strong winds can influence the abundance and activity of insects (Erkert 1982). The results from the Auwahi Wind Energy facility are mostly consistent with these trends, although nearly one-fifth of our bat observations were made when wind speeds were greater than the mitigation cut-in speed of 6.9 m/sec. When we modeled the influence of environmental conditions on the probability of hoary bats occurring at the Auwahi Wind Energy facility, results revealed that bat occurrence was negatively related to wind speed, averaged over 10-minute intervals, and possibly declined after or during rain events (although available precipitation data made it difficult to clearly test for the influence of rain at the nightly temporal scale we used for the analysis). Despite the apparent relation of bat detection rates with wind speed and precipitation (both negative), the relation was not predictable—considerable variation was present in the modeled response of bats to weather. We found that low detection rates could occur when conditions appeared favorable, such as when there was no wind and wind speeds were low. Conversely, high detection rates may occur during relatively unfavorable conditions. For example, the largest observed detection rate we documented (nearly a bat per hour) occurred on the night of 15 November when turbine blade rotation averaged 7.1 rpm, wind speed averaged 5.7 m/sec, and wind speed variability, blade rotation intermittency, and light precipitation were also similar to the average conditions observed during the entire four-month study period. Such an event does not seem predictable

given available information, but this does not mean that predictable associations among bat occurrence, environmental conditions, and turbine operation do not exist.

Our study objective was to learn more about how bat behaviors at wind turbines relate to wind speed and turbine operation—key elements of effective mitigation strategies for minimizing fatalities of Hawaiian hoary bats. In assessing possible reasons for bat occurrence near the turbines at the Auwahi Wind Energy facility during high wind conditions, we evaluated our data in the context of behaviors we observed on video and the unique turbine operational conditions observable due to the relatively high curtailment cut-in wind speed of 6.9 m/sec. One of the patterns that clearly emerged from the data was that bats were more likely to be detected at turbines when the blades were not moving or were moving slowly, although perhaps not proportional to what would be expected due to wind speed alone in part because of curtailment. However, it is noteworthy that the bat detection rate at the non-operational turbine (WTG2) was similar to the overall mean and not found to be significantly different from the other three operational turbines. This may indicate that fast turbine blade movement is not a causal factor related to the attraction of bats and their presence at turbines. Nevertheless, variability in wind speed and turbine blade rotation intermittency were both positively related to bat detection probability in our analysis. Nearly one-fifth of the observations of bats at the Auwahi Wind Energy facility turbines occurred during conditions when wind speeds exceeded the 6.9 m/sec threshold, indicating that responding to wind-speed alone may not maximize opportunities to produce energy and avoid bat fatalities. When discussing similar results from a video study of bat activity at wind turbines on the U.S. mainland, Cryan *et al.* (2014) speculated "…observations that tree bats show a tendency to closely investigate inert turbines and sometimes linger for minutes to perhaps hours (in the cases of clustered observations) highlight the plausibility of a scenario in which bats are drawn toward turbines in low winds, but sometimes remain long enough to be put at risk when wind picks up and blades reach higher speeds. Therefore, the frequency of intermittent, blade-spinning wind gusts within such low-wind periods might be an important predictor of fatality risk; fatalities may occur more often when turbine blades are transitioning from potentially attractive (stationary or slow) to lethal (fast) speeds."

Such a scenario may be compatible with our observations and analysis from the Auwahi Wind Energy facility. For example, of the proportionally small sample of 34 bat events we observed when turbine blades were moving more than one-half a rotation per minute, eight ensued when wind speeds were below the curtailment threshold. These events may have occurred because of computational lags over the 10-minute period within which the rolling average wind-speed calculated included occasional interludes during which winds dropped below the cut-in threshold but did not yet trigger curtailment. Combining these observations with earlier discussion that bats visiting the Auwahi Wind Energy facility might periodically and intensely search the turbines for feeding opportunities, a plausible hypothesis emerges: Hawaiian hoary bats might occur at the Auwahi Wind Energy facility during variable wind periods because windy periods concentrate insects on the lee of emergent features (e.g., trees), and when winds slacken bats might take the opportunity to focus foraging on the ephemeral concentrations of prey. In other words, relative to calm wind conditions, bats may opportunistically exploit certain landscape features during lulls on otherwise windy nights. A prerequisite for opportunistic use of tall structures such as wind turbines is that they be visually conspicuous and attract bats. This is largely supported by research demonstrating that, relative to surrounding landscapes, the activity of tree bats at tall structures increases as individuals encounter these features during migration in late summer and autumn (Jameson and Willis 2014).

Our study was not able to make optimal use of combined sampling methods because of the poor quality of acoustic data. Fortunately, video cameras functioned more consistently and produced more useful data for drawing inferences about bat presence and behaviors at the turbines than acoustic detectors. Known limitations of the acoustic detection process and potentially cryptic vocalization behavior of hoary bats were concerns going into this study, as well as likely only a modest overlap of the airspace sampled by the two methods (bats could be out of the video field of view, and video can also image farther than an acoustic detector can sample). In general, we confirmed that the range of acoustic detectors was different, less consistent across conditions, and generally lower than thermal surveillance cameras in this study. Although it is clear that Hawaiian hoary bats are acoustically active when present at Auwahi Wind Energy facility, it also appears that the species exhibits, to some extent, the cryptic vocalization noted in other settings (Gorresen *et al.* 2017, Corcoran and Weller 2018). Although both video and acoustic sampling had similar detection rates for the entire four-month monitoring period (albeit not directly comparable because acoustic sampling was weighted towards the earlier months during which nightly bat detections were more prevalent), there was a clear mismatch in the incidence and proportion of samples with bat detections. For the subset of concurrently sampled turbine-nights, acoustic detectors confirmed bat presence in about three-quarters of the turbine-nights for which bats were also detected by thermal cameras. Acoustic bat detectability further declined at finer-resolution time periods of sampling, such as hourly and 10-minute intervals at which video monitoring determined bat occurrence. The frequent lack of detections within a reasonable window for informing acoustically triggered turbine curtailment may have implications for the effectiveness of this method in reducing fatalities, at least in the setting examined in this study. The nature and variability of vocalization by bats at tall structures such as turbines, as well as the operational limits of the detection system, warrants further investigation using both acoustic and videographic methods.

ACKNOWLEDGEMENTS

For access, support, and logistics, we thank the staff at the Auwahi Wind Energy facility—M. VanZandt, G. Akau, B. Campbell, N. Santos, R. Pederson, and J. Galvan. We also thank C. Sutter and Natural Power Consultants, LLC, for providing acoustic files recorded at Auwahi Wind Energy. We are indebted to K. Brinck, K. Courtot, B. Straw, and S. Nash for review of the draft report. Supporting data are available at Gorresen 2020, https://doi.org/10.5066/P937H9LQ. Any use of trade, firm, or product names is for descriptive purposes only and does not imply endorsement by the U.S. Government.

LITERATURE CITED

Adams, A. M., M. K. Jantzen, R. M. Hamilton, and M. B. Fenton. 2012. Do you hear what I hear? Implications of detector selection for acoustic monitoring of bats. Methods in Ecology and Evolution 3:992–998.

Arnett, E. B., and E. F. Baerwald. 2013. Impacts of wind energy development on bats: implications for conservation. In: R. A. Adams, S. C. Peterson, editors. Bat evolution, ecology, and conservation. New York: Springer Science Press. Pp. 435–456.

Arnett, E. B., W. K. Brown, W. P. Erickson, J. K. Fiedler, B. L. Hamilton, T. H. Henry, A. Jain, G. D. Johnson, J. Kerns, R. R. Koford, and C. P. Nicholson. 2008. Patterns of bat fatalities

at wind energy facilities in North America. The Journal of Wildlife Management 72:61–78.

Baerwald, E. F., and R. M. Barclay. 2009. Geographic variation in activity and fatality of migratory bats at wind energy facilities. Journal of Mammalogy 90:1341–1349.

Bolker, B. M., and R Development Core Team. 2017. bbmle: tools for general maximum likelihood estimation. R package version 1.0.20. https://CRAN.R-project.org/package=bbmle

Brooks, M. E., K. Kristensen, M. R. Darrigo, P. Rubim, M. Uriarte, E. Bruna, and B. M. Bolker. 2019. Statistical modeling of patterns in annual reproductive rates. Ecology. p.e02706.

Burnham, K. P., and D. R. Anderson. 2002. Model selection and multi-model inference: a practical information-theoretic approach. Second edition. Springer-Verlag, New York, USA.

Burnham, K. P., D. R. Anderson, and K. P. Huyvaert. 2011. AIC model selection and multimodel inference in behavioral ecology: some background, observations, and comparisons. Behavioral Ecology and Sociobiology 65:23–35.

Byrne, S. 1983. Bird movements and collision mortality at a large horizontal axis wind turbine. Cal-Neva Wildlife Transactions. Pp. 76–83.

Corcoran, A. J., and T. J. Weller. 2018. Inconspicuous echolocation in hoary bats (*Lasiurus cinereus*). Proc R Soc B 285: 20180441. https://doi.org/10.1098/rspb.2018.0441 PMID: 29720417

Cryan, P. M., and R. M. R. Barclay. 2009. Causes of bat fatalities at wind turbines: Hypothesis and predictions. Journal of Mammalogy 90:1330–1340.

Cryan, P. M., P. M. Gorresen, C. D. Hein, M. R. Schirmacher, R. H. Diehl, M. M. Huso, D. T. S. Hayman, P. D. Fricker, F. J. Bonaccorso, D. H. Johnson, K. Heist, and D. C. Dalton. 2014. Behavior of bats at wind turbines. Proceedings of the National Academy of Sciences 111, 15126–15131. https://doi.org/10.1073/pnas.1406672111

Delacre, M., D. Lakens, and C. Leys. 2017. Why psychologists should by default use Welch's t-test instead of Student's t-test. International Review of Social Psychology 30:92-101.

Erickson, J. L., and S. D. West. 2002. The influence of regional climate and nightly weather conditions on activity patterns of insectivorous bats. Acta Chiropterologica 4:17–24.

Erkert, H. G. 1982. Ecological aspects of bat activity rhythms. In Ecology of bats (pp. 201-242). Springer, Boston, MA.

Fiedler, J. K. 2004. Assessment of bat mortality and activity at Buffalo Mountain windfarm, Eastern Tennessee. Thesis, University of Tennessee, Knoxville, USA.

Foo, C. F., V. J. Bennett, A. M. Hale, J. M. Korstian, A. J. Schildt, and D. A. Williams. 2017. Increasing evidence that bats actively forage at wind turbines. PeerJ 5:e3985. DOI 10.7717/peerj.3985

Gorresen, P. M. 2020. Hawaiian hoary bat (*Lasiurus cinereus semotus*) behavior at wind turbines, Maui Island 2018. U.S. Geological Survey data release https://doi.org/10.5066/P937H9LQ

Gorresen, P. M., K. W. Brinck, M. A. DeLisle, K. Montoya-Aiona, C. A. Pinzari, and F. J. Bonaccorso. 2018. Multi-state occupancy models of foraging habitat use by the Hawaiian hoary bat (*Lasiurus cinereus semotus*). PLoS ONE 13:e0205150.

Gorresen, P. M., P. M. Cryan, D. Dalton, S. Wolf, and F. J. Bonaccorso. 2015a. Ultraviolet vision may be widespread in bats. Acta Chiropterologica 17:193–198.

Gorresen, P. M., P. M. Cryan, M. M. Huso, C. D. Hein, M. R. Schirmacher, J. A. Johnson, K. M. Montoya-Aiona, K. W. Brinck, and F. J. Bonaccorso. 2015b. Behavior of the Hawaiian hoary bat (*Lasiurus cinereus semotus*) at wind turbines and its distribution across the North Koʻolau Mountains, Oʻahu. Technical Report HCSU-064.

Gorresen, P. M., P. M. Cryan, K. Montoya-Aiona, and F. J. Bonaccorso. 2017. Do you hear what I see? Vocalization relative to visual detection rates of Hawaiian hoary bats (*Lasiurus cinereus semotus*). Ecology and Evolution 7:6669–6679. https://doi.org/10.1002/ece3.3196 PMID: 28904749

Hartig, F. 2017. DHARMa: residual diagnostics for hierarchical (multi-level/mixed) regression models. R package version 0.1.5.

Hayes, M. A., L. A. Hooton, K. L. Gilland, C. Grandgent, R. L. Smith, S. R. Lindsay, J. D. Collins, S. M. Schumacher, P. A. Rabie, J. C. Gruver, and J. Goodrich-Mahoney. 2019. A smart curtailment approach for reducing bat fatalities and curtailment time at wind energy facilities. Ecological Applications 29:e01881.

Horn, J. W., E. B. Arnett, T. H. Kunz, 2008. Behavioral responses of bats to operating wind turbines. Journal of Wildlife Management 72:123–132. https://doi.org/10.2193/2006-465

Howell, J., and J. Didonato. 1991. Assessment of avian use and mortality related to wind turbine operations: Altamont Pass, Alameda and Contra Costa Counties. Final report to U.S. Windpower, Inc., Livermore, CA. P. 72.

Jameson, J. W., and C. K. Willis. 2014. Activity of tree bats at anthropogenic tall structures: implications for mortality of bats at wind turbines. Animal Behaviour 97:145–152.

Johnson, G. D. 2005. A review of bat mortality at wind-energy developments in the United States. Bat Research News 46:45–49.

Korner-Nievergelt, F., R. Brinkmann, I. Niermann, and O. Behr. 2013. Estimating bat and bird mortality occurring at wind energy turbines from covariates and carcass searches using mixture models. PLoS ONE 8:1–11.

Kunz, T. H., E. B. Arnett, B. M. Cooper, W. P. Erickson, R. P. Larkin, T. Mabee, M. L. Morrison, M. D. Strickland, and J. M. Szewczak. 2007. Assessing impacts of wind-energy development on nocturnally active birds and bats: a guidance document. The Journal of Wildlife Management 71:2449–2486.

Mykleseth, K. 2017. Wind farms killing more bats than expected. Honolulu Star Advertiser. 14 Jan 2017. Available from: http://www.wind-watch.org/news/2017/01/15/wind-farms-killing-more-bats-than-expected/

Pinzari, C., R. Peck, T. Zinn, D. Gross, K. Montoya-Aiona, K. Brinck, M. Gorresen, and F. Bonaccorso. 2019a. Hawaiian hoary bat (*Lasiurus cinereus semotus*) activity, diet and prey availability at the Waihou Mitigation Area, Maui. Hawai'i Cooperative Studies Unit Technical Report HCSU-090.

Pinzari, C., R. Peck, T. Zinn, D. Gross, K. Montoya-Aiona, K. Brink, M. Gorresen, and F. Bonaccorso. 2019b. Hawaiian hoary bat (*Lasiurus cinereus semotus*) activity, diet, and prey availability at the Waihou Mitigation Area, Maui. U.S. Geological Survey data release https://doi.org/10.5066/P9U0KRMY

R Core Team. 2018. R: A language and environment for statistical computing. R Foundation for Statistical Computing, Vienna, Austria. https://www.Rproject.org/.

Schirmacher, M. R., A. Prichard, T. Mabee, and C. D. Hein. 2018. Evaluating a novel approach to optimize operational minimization to reduce bat fatalities at the Pinnacle Wind Farm, Mineral County, West Virginia, 2015. An annual report submitted to NRG Energy and the Bats and Wind Energy Cooperative. Bat Conservation International, Austin, TX.

Tetra Tech, Inc. 2018. Auwahi Wind Farm - Habitat Conservation Plan - Draft Amendment. November 19, 2018. Prepared for Auwahi Wind Energy LLC. Maui, Maui County, HI.

Tetra Tech, Inc. 2019. Auwahi Wind Farm Habitat Conservation Plan FY 2019 Annual Report. Prepared for Auwahi Wind Energy, LLC. Maui, Maui County, HI.

Tomich, P. Q. 1986. Mammals in Hawai'i: a synopsis and notational bibliography. Bishop Museum Special Publication 76. Bishop Museum Press, Honolulu, HI.

Weller, T. J., and J. A. Baldwin. 2012. Using echolocation monitoring to model bat occupancy and inform mitigations at wind energy facilities. The Journal of Wildlife Management 76: 619–631.

Wellig, S. D., S. Nusslé, D. Miltner, O. Kohle, O. Glaizot, V. Braunisch, M. K. Obrist, and R. Arlettaz. 2018. Mitigating the negative impacts of tall wind turbines on bats: Vertical activity profiles and relationships to wind speed. PloS ONE 13:e0192493.

APPENDIX I

Table 1. Total nightly bat visual (video) and acoustic detection events and respective detection rates (combined and adjusted for sampling effort for all four turbines). Additional supporting information (including detection events by turbine) are available as a U.S. Geological Survey data release at https://doi.org/10.5066/P937H9LQ. Total daily precipitation (cm) obtained from weather station USGS 203721156151601 (Kepuni Gulch Rain Gage, Maui, Hawaii, located 7.3 km ENE from Auwahi Wind Energy, LLC, at 226 m above local mean sea level) is available at: https://waterdata.usgs.gov/nwis/inventory?agency_code=USGS&site_no=203721156151601; also available at https://doi.org/10.5066/F7P55KJN.

Date	Total visual detection events	Visual detection rate	Total acoustic detection events	Acoustic detection rate	Daily precipitation (cm)
8/1/2018	1	0.029	0	0.000	0.00
8/2/2018	13	0.378	0	0.000	0.00
8/3/2018	5	0.146	0	0.000	0.00
8/4/2018	2	0.058	0	0.000	0.00
8/5/2018	1	0.029	0	0.000	0.00
8/6/2018	10	0.224	0	0.000	0.00
8/7/2018	8	0.173	2	0.087	0.00
8/8/2018	1	0.029	0	0.000	0.00
8/9/2018	0	0.000	0	0.000	1.73
8/10/2018	2	0.111	2	0.058	0.00
8/11/2018	0	0.000	2	0.058	0.46
8/12/2018	0	0.000	0	0.000	0.00
8/13/2018	3	0.129	4	0.115	0.00
8/14/2018	15	0.644	16	0.458	0.00
8/15/2018	2	0.086	9	0.257	0.00
8/16/2018	11	0.290	14	0.400	0.00
8/17/2018	6	0.172	4	0.114	0.20
8/18/2018	0	0.000	0	0.000	0.00
8/19/2018	5	0.128	3	0.085	0.00
8/20/2018	10	0.283	10	0.284	0.00
8/21/2018	0	0.000	1	0.028	0.00
8/22/2018	0	0.000	0	0.000	0.81
8/23/2018	1	0.021	0	0.000	1.30

Date	Total visual detection events	Visual detection rate	Total acoustic detection events	Acoustic detection rate	Daily precipitation (cm)
8/24/2018	0	0.000	0	0.000	4.17
8/25/2018	0	0.000	0	0.000	2.29
8/26/2018	0	0.000	0	0.000	2.21
8/27/2018	0	0.000	0	0.000	0.13
8/28/2018	0	0.000	0	0.000	0.03
8/29/2018	4	0.112	5	0.140	0.00
8/30/2018	1	0.028	7	0.196	0.00
8/31/2018	3	0.085	3	0.084	0.00
9/1/2018	1	0.028	2	0.056	0.00
9/2/2018	5	0.208	6	0.167	0.00
9/3/2018	2	0.083	0	0.000	0.00
9/4/2018	5	0.208	2	0.055	0.00
9/5/2018	3	0.124	5	0.138	0.00
9/6/2018	1	0.031	4	0.111	0.00
9/7/2018	4	0.084	6	0.166	0.00
9/8/2018	4	0.110	9	0.248	0.00
9/9/2018	8	0.165	5	0.138	0.00
9/10/2018	8	0.165	5	0.137	0.00
9/11/2018	2	0.041	3	0.082	0.00
9/12/2018	0	0.000	0	0.000	4.47
9/13/2018	0	0.000	0	0.000	0.79
9/14/2018	1	0.028	0	0.000	0.00
9/15/2018	0	0.000	0	0.000	0.00
9/16/2018	4	0.109	0	0.000	0.00
9/17/2018	1	0.027	1	0.027	0.00
9/18/2018	5	0.135	3	0.081	0.00
9/19/2018	0	0.000	0	0.000	0.00
9/20/2018	0	0.000	0	0.000	0.00
9/21/2018	0	0.000	0	0.000	0.00
9/22/2018	0	0.000	0	0.000	0.00
9/23/2018	0	0.000	0	0.000	0.30
9/24/2018	2	0.054	1	0.020	0.97
9/25/2018	5	0.134	18	0.362	0.05

Date	Total visual detection events	Visual detection rate	Total acoustic detection events	Acoustic detection rate	Daily precipitation (cm)
9/26/2018	2	0.054	5	0.100	0.00
9/27/2018	2	0.080	6	0.160	0.46
9/28/2018	0	0.000	0	0.000	0.03
9/29/2018	6	0.160	6	0.160	0.05
9/30/2018	0	0.000	2	0.053	0.00
10/1/2018	1	0.027	0	0.000	0.00
10/2/2018	2	0.053	0	0.000	0.00
10/3/2018	5	0.132	0	0.000	0.00
10/4/2018	8	0.211	2	0.079	0.00
10/5/2018	1	0.023	0	0.000	0.89
10/6/2018	5	0.099	0	0.000	1.88
10/7/2018	0	0.000	0	0.000	5.79
10/8/2018	2	0.039	1	0.079	0.20
10/9/2018	12	0.236	3	0.236	0.00
10/10/2018	8	0.157	0	0.000	0.00
10/11/2018	1	0.020	1	0.079	0.00
10/12/2018	4	0.157	0	0.000	1.83
10/13/2018	1	0.026	0	0.000	0.08
10/14/2018	14	0.273	2	0.156	0.00
10/15/2018	13	0.253	9	0.703	0.00
10/16/2018	8	0.156	8	0.624	0.00
10/17/2018	6	0.117	2	0.156	0.00
10/18/2018	6	0.161	8	0.622	0.00
10/19/2018	5	0.098	2	0.155	0.00
10/20/2018	3	0.058	8	0.620	0.00
10/21/2018	11	0.213	7	0.542	0.00
10/22/2018	7	0.154	4	0.309	0.00
10/23/2018	0	0.000	0	0.000	0.00
10/24/2018	2	0.038	0	0.000	0.00
10/25/2018	1	0.019	0	0.000	0.00
10/26/2018	2	0.044	0	0.000	0.00
10/27/2018	2	0.038	0	0.000	0.03
10/28/2018	0	0.000	0	0.000	0.00

Date	Total visual detection events	Visual detection rate	Total acoustic detection events	Acoustic detection rate	Daily precipitation (cm)
10/29/2018	0	0.000	0	0.000	0.13
10/30/2018	3	0.076	1	0.076	0.10
10/31/2018	1	0.019	1	0.076	0.03
11/1/2018	4	0.076	1	0.076	0.00
11/2/2018	5	0.096	1	0.076	0.00
11/3/2018	0	0.000	0	0.000	0.20
11/4/2018	1	0.019	0	0.000	0.20
11/5/2018	8	0.152	1	0.076	0.00
11/6/2018	0	0.000	0	0.000	0.00
11/7/2018	0	0.000	0	0.000	0.00
11/8/2018	2	0.038	0	0.000	0.00
11/9/2018	3	0.077	1	0.075	0.00
11/10/2018	4	0.100	1	0.075	0.00
11/11/2018	6	0.113	0	0.000	0.00
11/12/2018	2	0.075	1	0.075	0.00
11/13/2018	1	0.025	0	0.000	0.00
11/14/2018	2	0.067	0	0.000	0.03
11/15/2018	18	0.369	1	0.075	0.23
11/16/2018	6	0.114	3	0.225	0.00
11/17/2018	0	0.000	0	0.000	0.00
11/18/2018	1	0.019	1	0.075	0.00
11/19/2018	6	0.149	1	0.075	0.00
11/20/2018	0	0.000	0	0.000	0.00
11/21/2018	0	0.000	0	0.000	0.00
11/22/2018	0	0.000	0	0.000	0.76
11/23/2018	0	0.000	0	0.000	0.00
11/24/2018	1	0.019	1	0.074	0.00
11/25/2018	4	0.085	0	0.000	0.00
11/26/2018	0	0.000	0	0.000	0.00
11/27/2018	1	0.025	0	0.000	0.00
11/28/2018	0	0.000	0	0.000	0.00
11/29/2018	0	0.000	1	0.074	0.18
11/30/2018	0	0.000	0	0.000	0.00

APPENDIX II

Table 1. Summary of the number of nightly visual (video) and acoustic bat detection events per turbine, detection rate (number of detection events per hour, calculated as the nightly total of events divided by sample duration at a turbine), and the nightly metrics of weather and turbine operation variables, including precipitation ("precip"; total in cm for a 24-hour midnight-to-midnight period centered on the day of the record), mean wind speed ("wind-mean"; calculated as the mean of 10-minute interval recordings), variability in wind speed ("wind-sd"; calculated as the standard deviation of 10-minute interval recordings), turbine blade movement ("rpm"; rotations per minute), and turbine starts ("rpm-starts"; calculated as the total of such events following one or more 10-minute intervals at which the blade was motionless). Values include minimum, 1st quartile, median, mean, 3rd quartile, and maximum. All weather and turbine operation variables used in regression analysis were standardized and centered on the variable mean (i.e., subtracting variable values by its grand mean and dividing by its standard deviation). See methods for description of data sources. Additional supporting information are available as a U.S. Geological Survey data release at https://doi.org/10.5066/P937H9LQ.

Values	Visual detection events	Visual detection rate	Acoustic detection events	Acoustic detection rate	Precip	Wind-mean	Wind-sd	Rpm	Rpm-starts
Min:	0.000	0.000	0.000	0.000	0.000	0.985	0.745	0.000	0.000
1Q:	0.000	0.000	0.000	0.000	0.000	3.865	1.570	0.160	1.000
Median:	0.000	0.000	0.000	0.000	0.000	7.098	2.125	4.293	2.000
Mean:	0.934	0.077	0.988	0.081	0.271	7.336	2.178	6.394	3.879
3Q:	1.000	0.087	1.000	0.077	0.030	10.252	2.676	13.020	5.000
Max:	12.000	0.899	14.000	1.125	5.790	21.021	4.886	16.210	21.000

APPENDIX III

Figures 1–6. Post-model-fitting diagnostics performed with the DHARMa package (Hartig 2017). Diagnostics demonstrated that the six top-ranked regression models (listed in Tables 5 and 6) met assumptions of uniformity (left panels) and did not exhibit zero inflation (right panels).

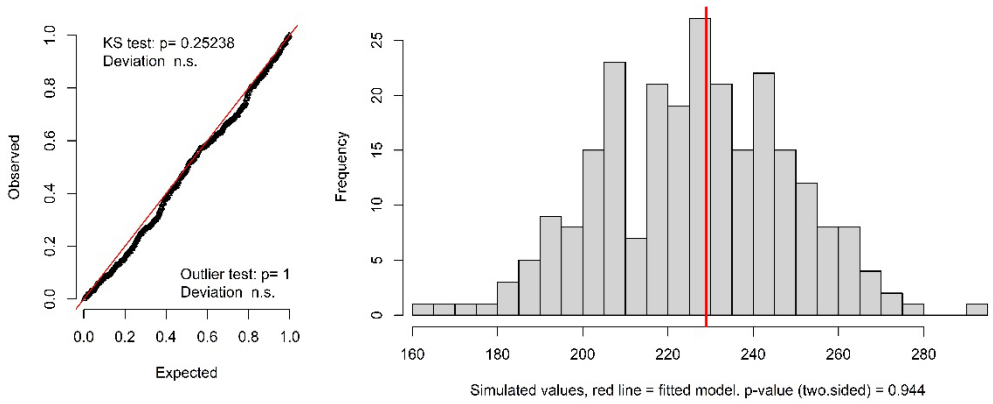

Figure 1. Model 1 of six top-ranked regression models. Left panel shows model met assumptions of uniformity, and right panel displays model did not exhibit zero inflation.

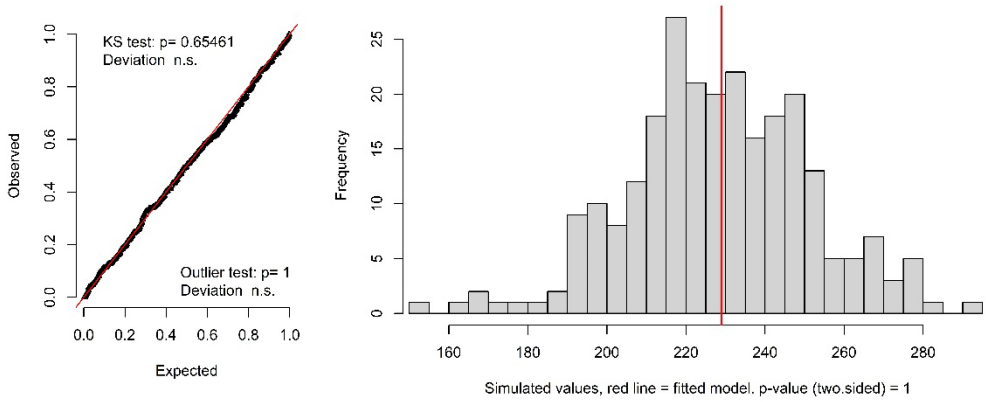

Figure 2. Model 2 of six top-ranked regression models. Left panel shows model met assumptions of uniformity, and right panel displays model did not exhibit zero inflation.

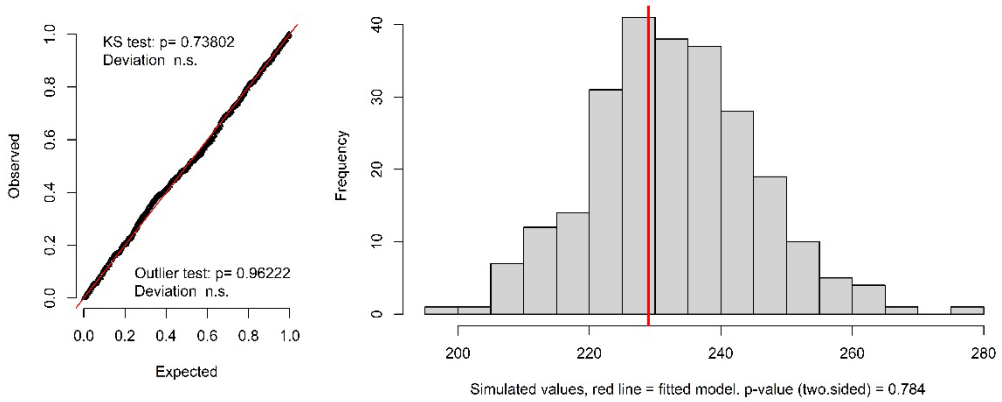

Figure 3. Model 3 of six top-ranked regression models. Left panel shows model met assumptions of uniformity, and right panel displays model did not exhibit zero inflation.

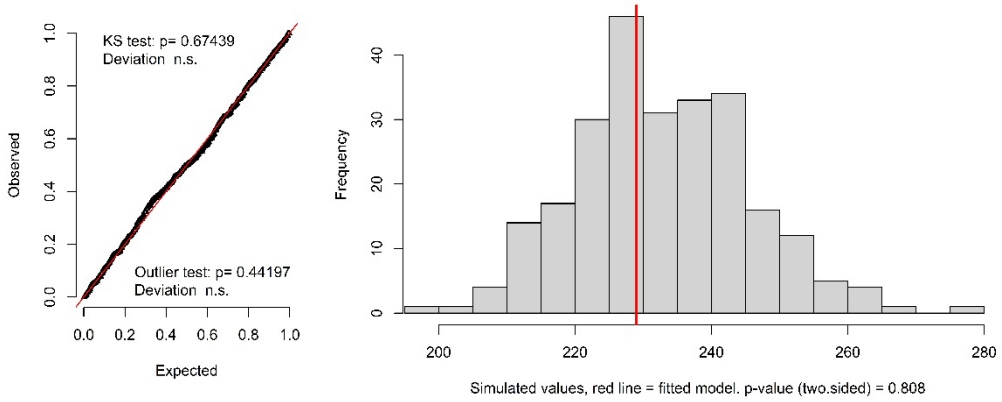

Figure 4. Model 4 of six top-ranked regression models. Left panel shows model met assumptions of uniformity, and right panel displays model did not exhibit zero inflation.

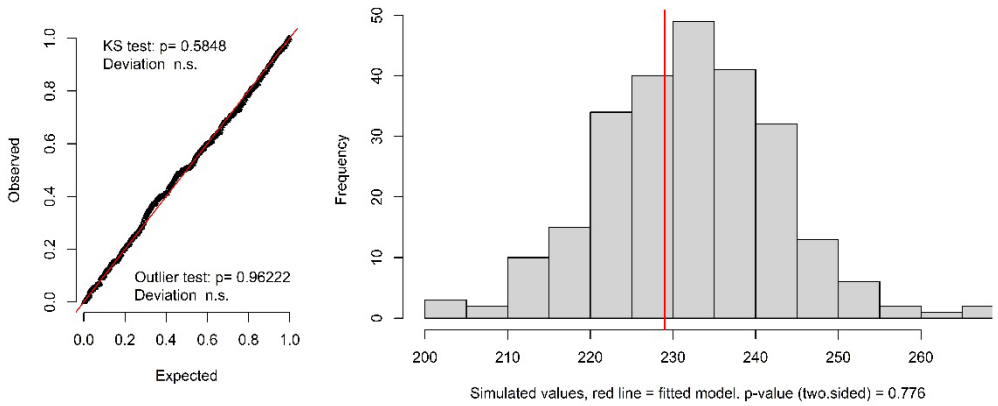

Figure 5. Model 5 of six top-ranked regression models. Left panel shows model met assumptions of uniformity, and right panel displays model did not exhibit zero inflation.

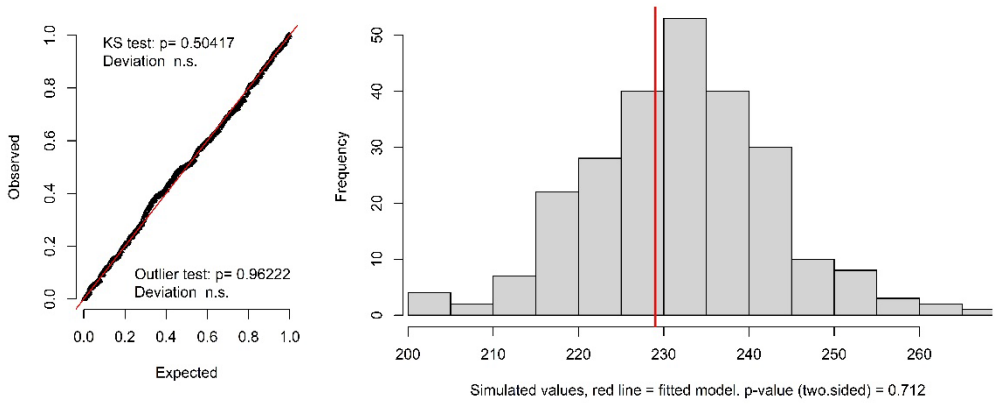

Figure 6. Model 6 of six top-ranked regression models. Left panel shows model met assumptions of uniformity, and right panel displays model did not exhibit zero inflation.